This is to certify that the

thesis entitled

FROM REGULATION TO CATALYSIS
A STUDY OF THE
ADP-GLUCOSE PYROPHOSPHORYLASE ENZYME

presented by

Jeremiah B. Frueauf

has been accepted towards fulfillment
of the requirements for

M.S. degree in Biochemistry and
Molecular Biology

Jack Preiss

Major professor

Date August 24, 2001

FROM REGULATION TO CATALYSIS: A STUDY OF THE ADP-GLUCOSE PYROPHOSPHORYLASE ENZYME

By

Jeremiah Benjamin Frueauf

A THESIS

Submitted to

Michigan State University

in partial fulfillment of the requirements

for the degree of

MASTER OF SCIENCE

Department of Biochemistry and Molecular Biology

2001

ABSTRACT

FROM REGULATION TO CATALYSIS: A STUDY OF THE ADP-GLUCOSE PYROPHOSPHORYLASE ENZYME

By

Jeremiah Benjamin Frueauf

Surplus carbon and energy is stored as starch in plants and as glycogen in bacteria. The formation of these storage polysaccharides begins with the synthesis of the sugar-nucleotide donor, ADP-glucose, by the enzyme ADP-glucose pyrophosphorylase. The enzyme has been characterized from many sources, providing much information about its properties. The ADP-glucose pyrophosphorylases from cyanobacteria are allosterically regulated, with activation by 3-phosphoglycerate and inhibition by orthophosphate. Arginine residue 294 was previously found to be involved in the inhibition of the ADP-glucose pyrophosphorylase from *Anabaena* PCC 7120. Site-directed mutagenesis of this residue was performed to further analyze the interaction with orthophosphate. We found that neither the size nor the charge of arginine residue 294 plays a specific role in orthophosphate binding and that a few of the mutants had an altered inhibitor specificity

Prediction of secondary structures and sequence alignment by computer software has assisted us in elucidating a few very highly conserved residues throughout ADP-glucose pyrophosphorylases. Site-directed mutagenesis of one of these residues in the enzyme from *Escherichia coli* was done to analyze its function. We found that aspartic acid residue 142 is involved in the catalysis of the *E. coli* enzyme and that a negative charge is necessary for effective catalysis to occur.

To my great, great Aunt Desi

ACKNOWLEDGMENTS

First, I would like to thank my advisor, Dr. Jack Preiss, for his guidance in the pursuit of my degree. I learned many lessons related to research and life while in his laboratory, many of which I will likely not fully appreciate until the later years of my life.

I would also like to thank my committee members, Drs. Cristoph Benning and Lee Kroos, for their insight and critical review of my research and my first opus, which is presented in the following pages.

I also want to acknowledge the contribution of my co-worker, Dr. Miguel Ballicora, to my educational experience while in Jack's laboratory. He was and always is willing to share his insight and perspectives about everything from making an assay virtually devoid of experimenter error to relating our subject of study to everyday life. In fact, I had no idea that I would learn so much about Argentina studying ADP-glucose pyrophosphorylase. Thanks.

I need to thank my family, especially my mom and dad, for their constant support of my every endeavor and for providing me with the opportunity to explore all that life has to offer.

Last but not least by any means, I would like to thank my wife Anastazia for her love and for always believing in me. Without her support and compassion, achieving my goals would not be as easy.

TABLE OF CONTENTS

LIST OF TABLES

LIST OF FIGURES

LIST OF ABBREVIATIONS

ADP-Glc: ADP-glucose
ADP-Glc PPase: ADP-glucose pyrophosphorylase
PP_i: Pyrophosphate
Glc-1-P: Glucose-1-phosphate
FBP: Fructose-1,6-bisphosphate
3PGA: 3-phosphoglycerate
P_i: Orthophosphate
PLP: Pyridoxal-5-phosphate
DTT: Dithiothreitol
BSA: Bovine serum albumin
HEPES: *N*-2-Hydroxyethylpiperazine-N'-ethanesulfonic acid
EDTA: Ethylenediaminetetracetic acid
IPTG: Isopropyl-β-D-thiogalactoside
PHD: Profile neural network
HCA: Hydrophobic Cluster Analysis
RmlA: dTDP-glucose pyrophosphorylase
GlmU: *N*-acetlyglucosamine 1-phosphate uridyltransferase

CHAPTER 1

LITERATURE REVIEW

1. Sugar-Nucleotides as Precursors to Carbohydrates

Living organisms convert surplus carbon and energy into storage polysaccharides when the supply exceeds the demand. Then when the supply becomes restricted, the stored carbohydrates can be utilized. Starch and glycogen, polysaccharides found in many organisms, make ideal candidates for storage reserves because of physical properties that allow for a low cellular osmotic pressure and a rapid metabolism (1,2).

The role sugar-nucleotides play in the biosynthesis of polysaccharides was first elucidated in the 1950's by Leloir and co-workers. They isolated and characterized the sugar-nucleotide UDP-D-glucose (UDP-Glc, (3,4)), laying the groundwork for the eventual establishment of sugar-nucleotides as glycosyl donors in polysaccharide synthesis (5,6). Since these pioneering studies, many sugar-nucleotides have been isolated and studied (7,8). This class of compounds is defined as a sugar or a sugar derivative attached by a glycosidic hydroxyl to the β phosphate of a nucleoside 5'-diphosphate (8) and are typically formed by the following general reaction:

$$\text{NTP} + \text{sugar-1-phosphate} \Leftrightarrow \text{NDP-sugar} + \text{inorganic pyrophosphate}$$

2. Starch

2.1 Properties and Localization of Starch

A majority of green plants contain starch, which is present throughout many plant tissues and organs such as leaves, stems, roots, fruits, grains, shoots and seeds. Isolation of starch from these sources provides a white, powdery solid with low solubility that has myriad industrial and commercial uses (9,10).

1. Sugar-Nucleotides as Precursors to Carbohydrates

Living organisms convert surplus carbon and energy into storage polysaccharides when the supply exceeds the demand. Then when the supply becomes restricted, the stored carbohydrates can be utilized. Starch and glycogen, polysaccharides found in many organisms, make ideal candidates for storage reserves because of physical properties that allow for a low cellular osmotic pressure and a rapid metabolism (1,2).

The role sugar-nucleotides play in the biosynthesis of polysaccharides was first elucidated in the 1950's by Leloir and co-workers. They isolated and characterized the sugar-nucleotide UDP-D-glucose (UDP-Glc, (3,4)), laying the groundwork for the eventual establishment of sugar-nucleotides as glycosyl donors in polysaccharide synthesis (5,6). Since these pioneering studies, many sugar-nucleotides have been isolated and studied (7,8). This class of compounds can be defined as a sugar or a sugar derivative attached by a glycosidic hydroxyl to the β-phosphate of a nucleoside 5'-diphosphate (8) and are typically formed by the following general reaction:

$$\text{XTP} + \text{sugar-1-phosphate} \Leftrightarrow \text{XDP-sugar} + \text{inorganic pyrophosphate}$$

2. Starch

2.1 Properties and Localization of Starch

A majority of green plants contain starch, which is present throughout many plant tissues and organs such as leaves, stems, roots, fruits, grains, shoots and seeds. Isolation of starch from these sources provides a white, powdery solid with low solubility that has myriad industrial and commercial uses (9,10).

Starch consists of two types of polyglucans, amylose and amylopectin (10,11). Amylose is a mainly linear molecule of α-1,4-linkages, with an average length of 10^3 residues and a few infrequent α-1,6-branch points. Amylopectin, a much larger molecule, has an average length of 10^4-10^5 residues. Each polymer of amylopectin is about 5% α-1,6-branched linkages, on average 20-24 glucose units in length per branch.

The formation and degradation of starch in plant leaves and other photosynthetic tissue proceeds entirely within the chloroplast (12,13). The starch formed through CO_2 fixation during the day is subsequently degraded by respiration to form sucrose at night. This delicate cycle controls the metabolic flux of energy throughout the plant. The sucrose that is made via the chloroplasts is then circulated to the non-photosynthetic tissues such as seeds, where the process of starch synthesis can be repeated in the amyloplast. The amyloplast is an organelle that resembles the chloroplast; however, not as much is known about the metabolism of the amyloplast. For example, the location of the starch biosynthetic enzymes and how the carbon source enters the organelle are still under consideration (2,13).

2.2 Synthesis of Starch

The biosynthesis of starch in plants begins with the formation of the donor molecule, ADP-glucose (Equation (1)), by the enzyme ADP-glucose pyrophosphorylase (ATP: α-D-glucose-1-phosphate adenyltransferase). This reaction is reversible; thus the enzyme has been labeled as either ADP-glucose synthetase for the synthesis of ADP-glucose (ADP-Glc) or ADP-glucose pyrophosphorylase (ADP-Glc PPase) for the pyrophosphorolysis of ADP-Glc. What occurs next is the transfer of the glucosyl unit from ADP-glucose to the glucan primer (Equation (2)). This reaction is catalyzed by

starch synthase (ADP-glucose: α-1,4-D-glucan-4-α-glucosyl transferase). The last reaction that takes place in starch synthesis (Equation (3)) is the rearrangement of the oligosaccharide by branching enzyme (1,4-α-D-glucan 6-α-(1,4-α-glucano)-transferase).

(1) $ATP + \alpha\text{-glucose-1-P} \Leftrightarrow ADP\text{-glucose} + PP_i$

(2) $ADP\text{-glucose} + glucan \Rightarrow \alpha\text{-1,4-glucosyl-glucan} + ADP$

(3) $\alpha\text{-1,4-oligosaccharide chain-glucan} \Rightarrow \alpha\text{-1,4-}\alpha\text{-1,6-branched-glucan}$

Some other enzymes, such as a debranching enzyme, have been isolated from the starch granule, which is contained within the amyloplast. These enzymes are proposed to further modify the starch end product by affecting its polysaccharide components amylose and amylopectin (11,14).

3. Glycogen

3.1 Properties and Purpose of Glycogen

Glycogen is the main storage polymer in many animal, fungal, and bacterial species. Of these three glycogen sources, much less is known about the structures of glycogen from fungi and bacteria; however, they do retain similarity to mammalian glycogen (15). In the case of bacterial glycogen, around 8-10% of the linkages are α-1,6, with an average chain length of 10-13 units. The glycogen polymer is on average 10^4 residues in length (1,16).

Glycogen typically accumulates in bacteria during the stationary phase of the growth cycle, when growth of the cell slows due to the lack of a nutrient, such as nitrogen, sulfur, or phosphate, and there is an excess supply of carbon (16-18). As an

example, in *Escherichia coli* B Holme showed that the quantity of glycogen accumulation was inversely proportional to the growth rate with glucose as the carbon source and the media lacking nitrogen (19). So, bacteria do not require glycogen for growth, but when alternative carbon sources are lacking and conditions are not favorable, glycogen likely helps preserve cell integrity (20).

Glycogen accumulation in cyanobacteria is a light-dependent process, occurring through oxygenic photosynthesis and under conditions of energy excess (21). In spite of this chloroplast-type of photosynthesis, cyanobacteria are prokaryotic organisms with characteristics typical of other prokaryotes, such as no internal compartmentalization (22). The convenience of working with prokaryotic organisms makes cyanobacteria ideal to study such processes as oxygen-evolving photosynthesis and its related effects, e.g. synthesis of storage polysaccharides. As will be discussed, the ADP-Glc PPases from cyanobacteria share many properties with the same protein from other bacteria and from plants.

3.2 Synthesis of Glycogen

In contrast to the structure, the biosynthesis of bacterial glycogen is different from mammals, including the glucosyl donor (UDP-Glc) and the regulation (23,24). The glucosyl donor for glycogen synthesis in bacteria is ADP-Glc, similar to plants. This was first demonstrated by Sigal *et al.* in *E. coli* mutants deficient in UDP-glucose pyrophosphorylase that still accumulated normal amounts of glycogen (25). The enzymes and reactions that form glycogen in bacteria are essentially the same as those that form starch in plants, with the key exception being the difference in end products. The enzyme catalyzing the formation of ADP-Glc (Equation (1)) is the same as in plants,

ADP-Glc PPase. Equations (2) and (3) are catalyzed by bacterial glycogen synthase and bacterial branching enzyme, respectively. Though these two enzymes catalyze similar reactions to their plant counterparts, either they must interact differently with the glucan or the branching enzymes must have different specificities in order to form glycogen instead of starch.

It is important to note that other pathways exist that lead to the formation of α-glucans in bacteria through the action of such enzymes as amylosucrase, amylomaltase and glycogen phosphorylase (26-28). However, much experimental evidence has been collected indicating that the main pathway is through the action of ADP-Glc PPase (2,16).

4. ADP-glucose Pyrophosphorylase

As stated above, both plant and bacterial organisms contain ADP-Glc PPase, which is the main regulatory step in the biosynthesis of their respective polysaccharide storage molecules (29). The sole physiological function of ADP-Glc in these organisms is as a glucose donor for glucan synthesis. It is therefore advantageous for the rate-limiting step to occur in response to the availability of ATP, a compound necessary for many cellular processes (2).

Since the isolation and identification of an ADP-Glc PPase from wheat by Espada in 1962 (30), many properties and aspects of this enzyme have been characterized from several organisms.

4.1 Properties of ADP-glucose Pyrophosphorylase

A majority of the ADP-Glc PPase enzymes from bacteria, cyanobacteria, and plants are allosteric and are regulated by the glycolytic intermediates of the major

pathways of carbon assimilation in each. Thus, the control of glycogen and starch synthesis is not only modulated by the availability of ATP, but by the accumulation of metabolic intermediates as well.

The ADP-Glc PPase enzymes studied to date are classified according to major and minor activators (Table I). For the enzymes from bacteria, these specificities divide the organisms into several classes. Although Table I does not represent all of the bacterial ADP-Glc PPases examined thus far, it does include organisms from a variety of metabolic backgrounds, e.g. photosynthetic and non-photosynthetic. An important observation to gather from this data is how the specificity of the activators overlaps between the groups (Table I). This suggests that the ADP-Glc PPases from these bacterial organisms share similar activator-binding sites. It is possible that mutation of the activator-binding site has occurred during evolution, allowing the specificity to adapt to the major metabolic pathway of the organism (13). The divergence is supported by data from alignment of the deduced amino acid sequences of many of these enzymes, which show that the regions of sequence encompassing substrate-binding residues are highly conserved whereas the activator-binding sites are less conserved (31).

Another observation is that the enzyme from *Serratia marcescens* is not activated by any metabolite tested (Table I, (32)). However, kinetic studies indicate there is an interaction between the substrate ATP and the inhibitor AMP, suggesting this ADP-Glc PPase is controlled by the energy charge (ATP-AMP ratio) of the cell. This concept of energy charge was first introduced for the *E. coli* ADP-Glc PPase enzyme by Shen and Atkinson (33). This ATP-AMP ratio helps regulate the synthesis of ADP-Glc and as stated above, controls the switch for the cell to begin the synthesis of glycogen.

Table 1. Comparison of the allosteric effectors for different ADP-glucose pyrophosphorylases

Source	Major Activator(s)	Minor Activator(s)	Inhibitor(s)
Escherichia coli (31) *Salmonella typhimurium* (32)	Fructose-1,6-bisphosphate Pyridoxal-5-phosphate NADPH	2-phosphoglycerate 3-phosphoglyceraldehyde Phosphoenolpyruvate	AMP
Rhodobacter spheroides (33) *Rhodobacter gelatinosa* (33)	Pyruvate Fructose-6-phosphate Fructose-1,6-bisphosphate		Orthophosphate
Agrobacterium tumefaciens (34) *Rhodobacter capsulata* (34)	Pyruvate Fructose-6-phosphate	2-deoxyribose 5-phosphate	AMP ADP Orthophosphate
Aeromonas hydrophila (35)	Fructose-6-phosphate Fructose-1,6-bisphosphate		ADP
Rhodospirillum rubrum (36)	Pyruvate		None
Serratia marcescens (37)	None		AMP
Plants (12) Green Algae (38) *Anabaena* PCC 7120 (39)	3-phosphoglycerate	Fructose-6-phosphate Fructose-1,6-bisphosphate	Orthophosphate

ADP-Glc PPases isolated from cyanobacteria, green algae, and plants are activated by 3-phosphoglycerate (Table I, (13)). These glycogen and starch synthesizing organisms are allosterically controlled by the primary CO_2 fixation product of photosynthesis. The major activator of these organisms is 3-phosphoglycerate (3PGA); however, other compounds have been found to activate the enzyme from plants, such as fructose-1,6-bisphosphate (FBP) for ADP-Glc PPase from spinach (*Spinacia oleracea*) leaf. Almost 3-fold more FBP than 3PGA is required to effect 50% of the maximal stimulation at pH 8.5 (42). Though 3PGA is a more efficient activator, the fact that another compound can activate this enzyme from spinach leaf supports this divergence of activator-binding sites.

The inhibitors of the enzymes from the sources obtained thus far include AMP, ADP, and orthophosphate (P_i), all of which are involved in energy metabolism. The ADP-Glc PPases from bacteria are generally more sensitive to AMP and ADP, while those from cyanobacteria, green algae, and plants are susceptible to P_i (Table I). Just as there are no activators for some of the bacterial ADP-Glc PPases, there are a few bacterial enzymes that are not inhibited by any of the above compounds, e.g. *Rhodospirillum rubrum* (38).

Another property of ADP-Glc PPases is that they require a divalent cation for the synthesis or pyrophosphorolysis of ADP-Glc. In the enzyme from *E. coli*, Mg^{2+} is most effective at fulfilling the requirement, however Mn^{2+} and Co^{2+} are able to replace Mg^{2+} (34). An interesting observation is that for maximal activity of the enzyme, the Mg^{2+} concentration needed to be 2- to 3-fold in excess of the ATP concentration, whereas the Mn^{2+} concentration needed to be 1:1 with ATP (43). This suggests that for optimal

activity of the ADP-Glc PPase, Mg^{2+} is interacting directly with the enzyme, in addition to the interaction between the divalent cation, the ATP, and the enzyme.

4.2 Subunit Structure of ADP-glucose Pyrophosphorylase

The subunit structure of ADP-Glc PPases from bacteria is homotetrameric (α_4), each subunit having a molecular mass of about 50 kDa (2). These molecular weights were estimated using sedimentation equilibrium ultracentrifugation of purified enzymes from *E. coli* B (44,45) and *R. rubrum* (38) and sucrose gradient ultracentrifugation of partially to fully purified enzymes from several other bacterial species (46). Sequencing of the ADP-Glc PPase genes from *E. coli* and *Rhodobacter sphaeroides*, which were isolated and sub-cloned (47,48), support the molecular weight estimation, as the deduced amino acid sequences give a molecular weight for the proteins of 48,762 and 47,312 kDa, respectively (49,48).

Similar to the enzymes from bacteria, the ADP-Glc PPase enzymes from cyanobacteria are homotetrameric in structure. Molecular weight determination by SDS-polyacrylamide gel electrophoresis of the highly purified enzymes from *Anabaena* PCC 7120 and *Synechocystis* PCC 6803 give masses of 50 and 53 kDa, respectively (41). The deduced amino acid sequences from the cloned ADP-Glc PPase genes of *Anabaena* (50) and *Synechocystis* (51) give values of 48,347 and 48,180 kDa, respectively, similar to the masses obtained from bacteria.

In contrast to ADP-Glc PPase enzymes from bacteria and cyanobacteria, the subunit structure of these enzymes in plants is heterotetrameric ($\alpha_2\beta_2$). The purified enzyme from spinach leaf revealed two different subunits with molecular masses of 51 and 54 kDa (40,52), designated as "small" and "large" based on the difference in size.

Other ADP-Glc PPases from plants have been studied, also indicating two dissimilar subunits of 55 and 60 kDa for maize (*Zea mays*) endosperm (53) and 50 and 51 kDa for potato (*Solanum tuberosum* L.) tuber (54). Data from amino-terminal sequencing, tryptic digests and immunological reactivity indicate that these subunits are the products of two separate genes (55) and suggest that they each have a specific role in the function of ADP-glucose pyrophosphorylase.

4.3 Comparison of ADP-glucose Pyrophosphorylase Protein Sequences

Alignment of the protein sequences of ADP-Glc PPases from bacteria shows strong identity (>80%); however, when comparing these enzymes with the protein sequences of the small and large subunits from plants, the identity drops to around 30% (Smith-White). Alignment of the small subunits from the various plant ADP-glucose pyrophosphorylases indicates good identity (>85%), in contrast to the comparison of only the large subunits (50-60%) or of the small and large subunits (40-60%, (31)). The high similarity of the small subunits is supported by the strong reaction of the antibody from the small subunit of spinach leaf with the corresponding ADP-Glc PPase subunit from rice (*Oryza sativa*) seed (56,57), maize endosperm (53,58), *Arabidopsis thaliana* leaf (59), and potato tuber (54). The lower homology between the small and large subunits reinforces the biochemical data suggesting that there was a gene duplication and divergence that produced two separate genes (55). Also, this low homology and that of the large-and-large comparisons implies that there is a tissue-specific regulation that the large subunit imparts upon the heterotetrameric enzyme. A study by Krishnan *et al.* confirmed that there are tissue-specific isozymes of ADP-Glc PPase isolated from the leaf and endosperm tissues of wheat, rice, and maize (56). Moreover, Morell *et al.*

showed that some epitopes are shared between the small and large subunits while others are unique only to the large subunit (52).

The overall homology between subunits of the various ADP-Glc PPases varies, but the similarity can be increased when comparing specific regions of the protein sequence. Presented in Figure 1 is an alignment of ADP-Glc PPases from bacteria (*E. coli*), cyanobacteria (*Anabaena*), and plants (potato tuber small and large subunits). The residues highlighted in bold typeface indicate absolute homology between the four groups. The alignment illustrates the low overall identity discussed above, but it also shows that among the groups there are a number of conservative substitutions (Figure 1). The alignment is also representative of the high sequence identity shared between cyanobacteria and higher plants, which coincides with the strong cross-reactivity of the cyanobacterial enzyme to the antibody prepared against the small subunit of spinach leaf (41). This information, along with that of the shared regulatory properties of plants and the shared homotetrameric structure of bacteria, demonstrates the unique relationship of cyanobacteria with bacteria and plants. Another aspect of the alignment that should be noted is the degree of conservation among specific regions of the sequence, e.g. the N-terminal sequence motif GG_GT(R/K), which is similar to the characteristic P-loop motif of nucleotide-binding proteins (60). As will be illustrated in the following section (section 4.4.1), some of these regions have been shown to play a role in substrate binding. In support of section 4.1, regions that have been shown to be important in the regulation of the ADP-Glc PPase are not conserved among all groups (Figure 1, within the non-bold typeface).

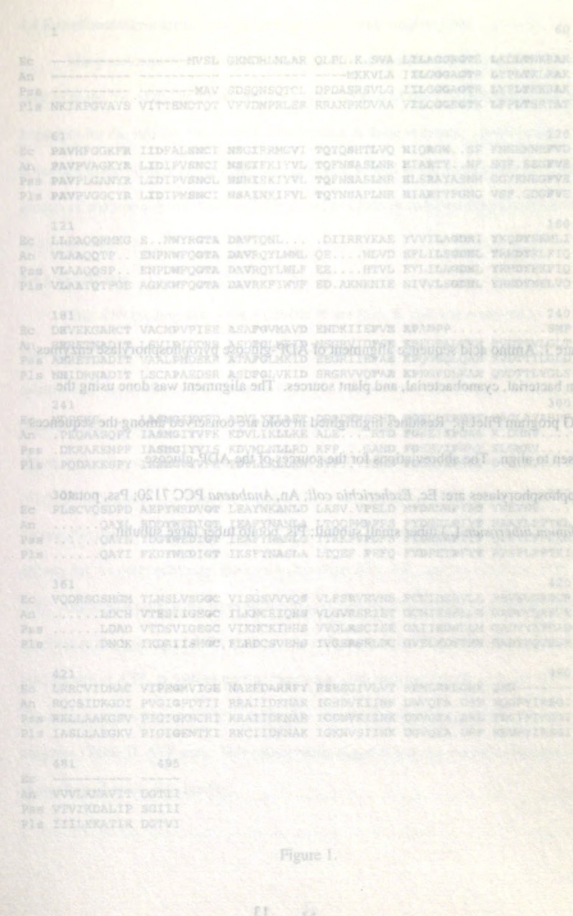

Figure 1.

Figure 1. Amino acid sequence alignment of ADP-glucose pyrophosphorylase enzymes from bacterial, cyanobacterial, and plant sources. The alignment was done using the GCG program PileUp. Residues highlighted in bold are conserved among the sequences chosen to align. The abbreviations for the sources of the ADP-glucose pyrophosphorylases are: Ec, *Escherichia coli*; An, *Anabaena* PCC 7120; Pss, potato (*Solanum tuberosum* L.) tuber small subunit; Pls, potato tuber large subunit.

```
    1                                                            60

Ec  ~~~~~~~~~~ ~~~~~~MVSL GKNDHLMLAR QLPL.K.SVA LILAGGRGTR LKDLTNKRAK
An  ~~~~~~~~~~ ~~~~~~~~~~ ~~~~~~~~~~ ~~~~MKKVLA IILGGGAGTR LYPLTKLRAK
Pss ~~~~~~~~~~ ~~~~~~MAV SDSQNSQTCL DPDASRSVLG IILGGGAGTR LYPLTKKRAK
Pls NKIKPGVAYS VITTENDTQT VFVDMPRLER RRANPKDVAA VILGGGEGTK LFPLTSRTAT

    61                                                           120

Ec  PAVHFGGKFR IIDFALSNCI NSGIRRMGVI TQYQSHTLVQ HIQRGW..SF FNEEMNEFVD
An  PAVPVAGKYR LIDIPVSNCI NSEIFKIYVL TQFNSASLNR HIARTY..NF SGF.SEGFVE
Pss PAVPLGANYR LIDIPVSNCL NSNISKIYVL TQFNSASLNR HLSRAYASNM GGYKNEGFVE
Pls PAVPVGGCYR LIDIPMSNCI NSAINKIFVL TQYNSAPLNR HIARTYFGNG VSF.GDGFVE

    121                                                          180

Ec  LLPAQQRMKG E..NWYRGTA DAVTQNL... .DIIRRYKAE YVVILAGDHI YKQDYSRMLI
An  VLAAQQTP.. ENPNWFQGTA DAVRQYLWML QE....WDVD EFLILSGDHL YRMDYRLFIQ
Pss VLAAQQSP.. ENPDWFQGTA DAVRQYLWLF EE....HTVL EYLILAGDHL YRMDYEKFIQ
Pls VLAATQTPGE AGKKWFQGTA DAVRKFIWVF ED.AKNKNIE NIVVLSGDHL YRMDYMELVQ

    181                                                          240

Ec  DHVEKGARCT VACMPVPIEE ASAFGVMAVD ENDKIIEFVE KPANPP.... .......SMP
An  RHRETNADIT LSVIPIDDRR ASDFGLMKID NSGRVIDFSE KPKGEALTKM RVDTTVLGLT
Pss AHRETDADIT VAALPMDEKR ATAFGLMKID EEGRIIEFAE KPQGEQLQAM KVDTTILGLD
Pls NHIDRNADIT LSCAPAEDSR ASDFGLVKID SRGRVVQFAE KPKGFDLKAM QVDTTLVGLS

    241                                                          300

Ec  NDPSKS.... LASMGIYVFD ADYLYELLEE DDRDENSSHD FGKDLIPKIT EAGLAYAHPF
An  .PEQAASQPY IASMGIYVFK KDVLIKLLKE ALE....RTD FGKEIIPDAA K.DHNV....
Pss .DKRAKEMPF IASMGIYVIS KDVMLNLLRD KFP...GAND FGSEVIPGAT SLGMRV....
Pls .PQDAKKSPY IASMGVYVFK TDVLLKLLKW SYP...TSND FGSEIIPAAI D.DYNV....

    301                                                          360

Ec  PLSCVQSDPD AEPYWRDVGT LEAYWKANLD LASV.VPELD MYDRNWPIRT YNEYNV....
An  ......QAYL FDDYWEDIGT IEAFYNANLA LTQQPMPPFS FYDEEAPIYT RARYLPPTKL
Pss ......QAYL YDGYWEDIGT IEAFYNANLG ITKKPVPDFS FYDRSAPIYT QPRYLPPSKM
Pls ......QAYI FKDYWEDIGT IKSFYNASLA LTQEF.PEFQ FYDPKTPFYT SPRFLPPTKI

    361                                                          420

Ec  VQDRSGSHGM TLNSLVSGGC VISGSVVVQS VLFSRVRVNS FCNIDSAVLL PEVWVGRSCR
An  ......LDCH VTESIIGEGC ILKNCRIQHS VLGVRSRIET GCMIEESLLM GADFYQASGI
Pss ......LDAD VTDSVIGEGC VIKNCKIHHS VVGLRSCISE GAIIEDSLLM GADYYETDAD
Pls ......DNCK IKDAIISHGC FLRDCSVEHS IVGERSRLDC GVELKDTFMM GADYYQTESE

    421                                                          480

Ec  LRRCVIDRAC VIPEGMVIGE NAEEDARRFY RSEEGIVLVT REMLRKLGHK QER~~~~~~~
An  RQCSIDKGDI PVGIGPDTII RRAIIDKNAR IGHDVKIINK DNVQEA.DRE SQGFYIRSGI
Pss RKLLAAKGSV PIGIGKNCHI KRAIIDKNAR IGDNVKIINK DNVQEA.ARE TDGYFIKSGI
Pls IASLLAEGKV PIGIGENTKI RKCIIDKNAK IGKNVSIINK DGVQEA.DRP EEGFYIRSGI

    481          495
Ec  ~~~~~~~~~~ ~~~~~
An  VVVLKNAVIT DGTII
Pss VTVIKDALIP SGIII
Pls IIILEKATIR DGTVI
```

Figure 1.

4.4 Functional/Structural Sites of ADP-glucose Pyrophosphorylase

Many techniques, including chemical modification and mutagenesis, have been used to probe the ADP-Glc PPase enzymes, with the goal of identifying residues that are important for the structural/functional relationships of these enzymes. Amino acids important in the binding of substrates and effectors, as well as those important for other aspects of enzyme activity, have been identified and help in understanding the dynamics of the enzyme.

4.4.1 Substrates

The ATP binding site of the ADP-Glc PPase from *E. coli* was analyzed by reaction with 8-azido-ATP and 8-azido-ADP-glucose, photoaffinity analogs of the substrates in the synthesis and pyrophosphorolysis directions, respectively. After tryptic digestion and isolation of the azido-labeled peptide by high performance liquid chromatography, amino acid sequencing indicated that Tyr^{114} was covalently modified (61,62). Subsequent site-directed mutagenesis of this residue to phenylalanine showed a decrease in the apparent affinity for ATP, but there was also a decrease in the apparent affinity for the other substrate, glucose-1-phosphate (Glc-1-P), and the activator, FBP (63). Although Kumar *et al.* were unable to conclude that this residue was specifically involved in the binding of ATP, these results indicate that Tyr^{114} must be located near the binding site of ATP, as well as near or interacting with the sites for Glc-1-P and FBP. The amino acids adjacent to Tyr^{114} are highly conserved among bacterial and plant enzymes (Table II, ATP site). This conservation suggests that the region is important in some facet of nucleotide-binding.

Table II. Conservation of amino acid sequence near substrate-interacting residues

Source	Glc-1-P site	ATP site
E. coli	FV**E**KP	W**Y**RGTADAV
Anabaena	FS**E**KP	WFQGTADAV
Spinach leaf small subunit	FA**E**KP	WFQGTADAV
Spinach leaf large subunit	FS**E**KP	WFQGTADAV
Potato tuber small subunit	FA**E**KP	WFQGTADAV
Potato tuber large subunit	FA**E**KP	WFQGTADAV

Another reagent, pyridoxal-5-phosphate (PLP), was used to study reactive lysines in the ADP-Glc PPase from *E. coli*. Upon reduction with $NaBH_4$, PLP forms a stable Schiff-base with lysines. The reaction of [^{3}H]PLP with the *E. coli* enzyme modified two lysines, Lys^{39} and Lys^{195} (64,65). The substrate ADP-Glc protected reaction of [^{3}H]PLP with Lys^{195}. Site-directed mutagenesis of this residue showed decreased affinity for Glc-1-P of 100- to 10,000-fold, while the other kinetic constants were unchanged (66). These results strongly support the involvement of Lys^{195} in the binding of Glc-1-P for the ADP-Glc PPase from *E. coli*. The other labeled residue, Lys^{39}, will be discussed in the next section (section 4.4.2).

E. coli residue Lys^{195} is conserved throughout ADP-Glc PPases from other bacterial sources, the small subunits of plants, and most of the large subunits of plants (Table II, Glc-1-P site). To test if a mutation of this residue in an ADP-Glc PPase from another source would have the same result as in *E. coli*, Fu *et al.* mutated the homologous residues in the subunits of the potato tuber enzyme, Lys^{198} (small) and Lys^{213} (large).

The Lys^{198} mutants showed similar results to the *E. coli* mutants, not affecting any kinetic constants besides the apparent affinity for Glc-1-P, which decreased 135- to 550-fold (67). In contrast, the Lys^{213} mutants showed no significant changes from the wild-type. These results indicate that Lys^{198} of the small subunit is involved in Glc-1-P binding, while Lys^{213} in the large subunit is not. Other results from a mutant of *A. thaliana* containing a tetramer of only the small subunit and from a recombinant tetrameric enzyme of small subunit from potato tuber demonstrated that in high concentrations of the activator, the small subunit had activity (68,69). These studies suggest that each subunit has a different role in the heterotetrameric enzyme: the small subunit is involved in substrate-binding (catalytic) while the large is involved in another aspect, such as allosteric regulation (regulatory).

4.4.2 Allosteric Effectors

As discussed above, pyridoxal-5-phosphate was used to probe lysines in the ADP-Glc PPase from *E. coli* and modified two lysyl residues (64,65). This reagent is an analog of FBP and has been shown to activate the ADP-Glc PPase from *E. coli* (64,70), so protection of Lys^{39} from [^{3}H]PLP binding by FBP was not surprising. Site-directed mutagenesis of this residue to glutamic acid by Gardiol and Preiss supported the prevention of label incorporation by FBP. The mutant showed a significant change in apparent affinity for just the activator, indicating that Lys^{39} interacts directly with FBP (71).

PLP is also an analog of the activator 3PGA, and it activates the ADP-Glc PPases from spinach leaf (72) and *Anabaena* (41). In ADP-Glc PPase from spinach leaf, PLP modified Lys^{440} of the small subunit and three lysyl residues in the large subunit, with

3PGA blocking the incorporation at these sites (72,73). The inhibitor P_i blocked incorporation at Lys^{440} of the small subunit (Table III, Site 2) and at one lysine of the large subunit (Table III, Site 1), suggesting that these two sites interact with the allosteric effectors.

Table III. Amino acid sequence alignment of activator binding sites for cyanobacterial and plant ADP-glucose pyrophosphorylases

Source	Site 1	Site 2
Anabaena	377-RAIID**K**NAR	414-IVVVL**K**NAVIT
Spinach leaf small subunit	398-RAIID**K**NAR	435-IVTVI**K**DALIP
Spinach leaf large subunit[a]	DAIID**K**NAR	ITVIF**K**QATIK
Potato tuber small subunit	399-RAIID**K**NAR	436-IVTVI**K**DALIP
Potato tuber large subunit	412-KCIID**K**NAK	450-IIILE**K**ATIRD

[a] A full length gene has not been isolated to assign numbers to this sequence.

In a similar experiment by Charng *et al.*, PLP modified Lys^{419} in the enzyme from *Anabaena*, which is homologous to Lys^{440} of the spinach leaf small subunit (Table III), with the activator blocking the incorporation. Site-directed mutagenesis of Lys^{419} showed decreased affinities (25- to 150-fold) for the activator 3PGA in the mutant enzymes, and reaction of the K419R mutant with PLP helped identify another lysyl residue involved in activator binding, Lys^{382} (Table III, (74)). Again, 3PGA blocked incorporation of PLP at Lys^{382}, and subsequent site-directed mutagenesis of this residue demonstrated decreases in apparent affinities for 3PGA of 10- to 160-fold compared to

the wild-type (75). These studies on the ADP-Glc PPase from *Anabaena* indicate that these lysines are important for the interaction of the enzyme with the allosteric activator 3PGA.

Since these lysyl residues are also conserved in the ADP-Glc PPase from potato tuber (Table III), Ballicora *et al.* mutated them to determine if the residues of both subunits are involved in the allosteric regulation of the enzyme. The data showed that each residue contributed to the binding of the activator 3PGA, but that the effect of mutation, i.e. the decrease in apparent affinity for 3PGA, on the small subunit residues was greater than the large subunit counterparts (76). These results indicate that in addition to a functional catalytic site, the small subunit also has a functional regulatory site. However, the affinity for 3PGA of the tetrameric enzymes containing the wild-type small subunit and either the wild-type or the mutants of the large subunit was similar (76). This suggests that the role of the large subunit is to modulate the regulation of the small subunit, which parallels the notion of tissue-specific regulation. In other words, the large subunit modulates the activity of the small subunit in the heterotetrameric enzyme based on the tissue-specific information it receives.

It seems that the residues involved in the activation of the ADP-Glc PPases from cyanobacteria and plants are in the C-terminal region, while in bacteria they appear to be in the N-terminal. However, there is recent evidence showing that both the N- and C-terminals are important for the regulation of the enzymes from all sources. For example, Ballicora *et al.* showed that the N-terminal of the small subunit from potato tuber is necessary for allosteric regulation. Characterization of the recombinant enzyme showed similar kinetic and regulatory properties to the enzyme purified directly from the

potato tuber (69). In comparison, the characterization of a recombinant enzyme missing 10 residues at the N-terminal of the small subunit showed about a 10-fold increase in apparent affinity for the activator 3PGA compared to the endogenous enzyme (69,77). Also, results from a study on chimeric enzymes between the ADP-Glc PPases from *E. coli* and *Agrobacterium tumefaciens*, where two-thirds of the enzyme containing the N-terminal and one-third of the enzyme containing the C-terminal were switched, demonstrated that the C-terminus of the *E. coli* enzyme was important for the FBP activator specificity (Ballicora, M. A., Iglesias, A. A., and Preiss, J., unpublished results).

The arginine-specific reagent phenylglyoxal has been used to probe the allosteric sites of the ADP-Glc PPases from spinach leaf (78) and cyanobacteria (41,79). Phenylglyoxal modification of these enzymes was prevented by addition of the activator 3PGA or of the inhibitor P_i. In the ADP-Glc PPases from cyanobacteria and plants there are five highly conserved arginine residues that are not present in the enzymes from enteric bacteria. Since the effector specificity is different between these groups, site-directed mutagenesis was performed to determine if these residues are involved in the allosteric regulation of the cyanobacterial enzyme. Sheng and Preiss mutated the conserved arginines to alanine and found with the R294A mutant that the apparent affinity for P_i decreased in the presence (38-fold) and absence (100-fold) of the activator, while the other kinetic constants were relatively unchanged (80). The results suggest that Arg^{294} of the ADP-Glc PPase from *Anabaena* interacts with the inhibitor P_i.

4.4.3 Activity Modulating Residues

A number of other ADP-Glc PPase mutants with altered allosteric properties have been studied (see (81-84)). These mutants did not demonstrate a specific role in the

interaction with any one particular ligand; however, they did seem to be involved in maintaining the "state" of the enzyme. Allosteric regulation modulates the enzyme through inactive and active states by switching through at least two conformations (85,86). It is possible then, that the residues in these regions of the ADP-Glc PPase enzyme are involved in the transition of the tertiary and quaternary structure to form the active state of the enzyme. Moreover, in a study by Wu and Preiss involving limited proteolysis of the ADP-Glc PPase from *E. coli*, an N- and C-terminal truncated enzyme demonstrated altered allosteric properties (87). This proteolyzed enzyme showed significant decreases in the ratio of activation for FBP and a decrease in sensitivity to the inhibitor AMP, making a highly active enzyme. Construction of an enzyme without the first eleven amino acids through recombinant DNA technology showed similar results as for the proteolyzed form (88), indicating that the C-terminal was not responsible for the change. Thus it seems that the N-terminal is also involved in maintaining the "state" of the enzyme. Current work in our laboratory on more N-terminal deletions of the ADP-Glc PPase from *E. coli* seems to indicate that the peptide between the first 10 to 20 amino acids is specifically involved in this switching (Hinz, A., Ballicora, M. A., and Preiss, J., unpublished results).

References

1. Candy, D. J. (1980) *Biological Functions of Carbohydrates*, Halsted Press, New York
2. Preiss, J., and Sivak, M. N. (1998) in *Comprehensive Natural Products Chemistry* (Pinto, B. M., ed) Vol. 3, pp. 441-495, Pergamon Press, Oxford
3. Cardini, C. E., Paladini, A. C., Caputto, R., and Leloir, L. F. (1950) *Nature* **165,** 191-192
4. Caputto, R., Leloir, L. F., Cardini, C. E., and Paladini, A. C. (1950) *J. Biol. Chem.* **184,** 333-350
5. Leloir, L. F., and Cabib, E. (1953) *J. Am. Chem. Soc.* **75,** 5445-5446
6. Glaser, L., and Brown, D. (1955) *Proc. Natl. Acad. Sci. U. S. A.* **41,** 253-260
7. Cabib, E. (1963) in *Annu. Rev. Biochem.* (Snell, E. E., Luck, J. M., Allen, F. W., and MacKinney, G., eds) Vol. 32, pp. 321-354, Annual Reviews, Inc., Palo Alto
8. Ginsburg, V. (1964) in *Adv. Enzymol.* (Nord, F. F., ed) Vol. 26, pp. 35-88, Interscience Publishers, Inc., New York
9. Kearsley, M. W., and Dziedzic, S. Z. (eds) (1995) *Handbook of Starch Hydrolysis Products and Their Derivatives*, The University Press, Cambridge
10. Schenck, F. W., and Hebeda, R. E. (eds) (1992) *Starch Hydrolysis Products: Worldwide Technology, Production, and Applications*, VCH Publishers, New York
11. Preiss, J., and Sivak, M. N. (1998) in *Genet. Eng. (N. Y).* (Setlow, J. K., ed) Vol. 20, pp. 177-223, Plenum Press, New York

12. Preiss, J. (1988) in *The Biochemistry of Plants* (Preiss, J., ed) Vol. 14, pp. 181-254, Academic Press, New York

13. Sivak, M. N., and Preiss, J. (1998) in *Adv. Food Nutr. Res.* (Taylor, S. L., ed) Vol. 41, pp. 1-199, Academic Press, San Diego

14. Ball, S., Guan, H. P., James, M., Myers, A., Keeling, P., Mouille, G., Buleon, A., Colonna, P., and Preiss, J. (1996) *Cell* **86,** 349-352.

15. Manners, D. J. (1971) in *The Yeasts* (Rose, A. H., and Harrison, J. S., eds) Vol. 2, pp. 419-439, Academic Press, New York

16. Preiss, J. (1984) *Annu. Rev. Microbiol.* **38,** 419-458

17. Dawes, E. A., and Senior, P. J. (1973) *Adv. Microb. Physiol.* **10,** 135-266

18. Preiss, J., and Romeo, T. (1989) *Adv. Microb. Physiol.* **30,** 183-238

19. Holme, T. (1957) *Acta Chem. Scand.* **11,** 763-775

20. Preiss, J. (1989) in *Bacteria in Nature* (Poindexter, J. S., and Leadbetter, E. R., eds) Vol. 3, pp. 189-258, Plenum, New York

21. Shively, J. M. (1988) *Methods Enzymol.* **167,** 195-203

22. Aitken, A. (1988) *Methods Enzymol.* **167,** 145-154

23. Cohen, P. (1986) in *The Enzymes* (Boyer, P. D., and Krebs, E. G., eds) Vol. 17, 3rd Ed., pp. 461-497, Academic Press, San Diego

24. Roach, P. J. (1986) in *The Enzymes* (Boyer, P. D., and Krebs, E. G., eds) Vol. 17, 3rd Ed., pp. 499-539, Academic Press, San Diego

25. Sigal, N., Cattaneo, J., and Segel, I. H. (1964) *Arch. Biochem. Biophys.* **108,** 440-451

26. Hehre, E. J. (1951) in *Adv. Enzymol.* (Nord, F. F., ed) Vol. 11, pp. 297-337, Interscience Publishers, Inc., New York

27. Hestrin, S. (1960) in *The Bacteria* (Gunsalus, I. C., and Stanier, R. Y., eds) Vol. 3, pp. 373-388, Academic Press, New York

28. Khandelwal, R. L., Spearman, T. N., and Hamilton, I. R. (1973) *Arch. Biochem. Biophys.* **154,** 295-305

29. Preiss, J. (1973) in *The Enzymes* (Boyer, P. D., ed) Vol. 8, pp. 73-119, Academic Press, New York

30. Espada, J. (1962) *J. Biol. Chem.* **237,** 3577-3581

31. Smith-White, B. J., and Preiss, J. (1992) *J. Mol. Evol.* **34,** 449-464

32. Ribereau-Gayon, G., Sabraw, A., Lammel, C., and Preiss, J. (1971) *Arch. Biochem. Biophys.* **142,** 675-692.

33. Shen, L. C., and Atkinson, D. E. (1970) *J. Biol. Chem.* **245,** 3996-4000.

34. Preiss, J., Shen, L., Greenberg, E., and Gentner, N. (1966) *Biochemistry* **5,** 1833-1845

35. Preiss, J., Greenberg, E., Parsons, T. F., and Downey, J. (1980) *Arch. Microbiol.* **126,** 21-31.

36. Eidels, L., Edelmann, P. L., and Preiss, J. (1970) *Arch. Biochem. Biophys.* **140,** 60-74.

37. Yung, S. G., Paule, M., Beggs, R., Greenberg, E., and Preiss, J. (1984) *Arch. Microbiol.* **138,** 1-8.

38. Furlong, C. E., and Preiss, J. (1969) *J. Biol. Chem.* **244,** 2539-2548.

39. Preiss, J., Crawford, K., Downey, J., Lammel, C., and Greenberg, E. (1976) *J. Bacteriol.* **127,** 193-203.

40. Sanwal, G. G., and Preiss, J. (1967) *Arch. Biochem. Biophys.* **119,** 454-469.

41. Iglesias, A. A., Kakefuda, G., and Preiss, J. (1991) *Plant Physiol.* **97,** 1187-1195

42. Ghosh, H. P., and Preiss, J. (1966) *J. Biol. Chem.* **241,** 4491-4504.

43. Gentner, N., and Preiss, J. (1968) *J. Biol. Chem.* **243,** 5882-5891.

44. Haugen, T., Ishaque, A., Chatterjee, A. K., and Preiss, J. (1974) *FEBS Lett.* **42,** 205-208.

45. Haugen, T. H., Ishaque, A., and Preiss, J. (1976) *J. Biol. Chem.* **251,** 7880-7885.

46. Preiss, J., and Walsh, D. A. (1981) in *Biology of Carbohydrates* (Ginsburg, V., ed) Vol. 1, pp. 199-314, Wiley, New York

47. Okita, T. W., Rodriguez, R. L., and Preiss, J. (1981) *J. Biol. Chem.* **256,** 6944-6952

48. Igarashi, R. Y., and Meyer, C. R. (2000) *Arch. Biochem. Biophys.* **376,** 47-58.

49. Baecker, P. A., Furlong, C. E., and Preiss, J. (1983) *J. Biol. Chem.* **258,** 5084-5088.

50. Charng, Y. Y., Kakefuda, G., Iglesias, A. A., Buikema, W. J., and Preiss, J. (1992) *Plant Mol. Biol.* **20,** 37-47

51. Kakefuda, G., Charng, Y. Y., Iglesias, A. A., McIntosh, L., and Preiss, J. (1992) *Plant Physiol.* **99,** 359-361

52. Morell, M. K., Bloom, M., Knowles, V., and Preiss, J. (1987) *Plant Physiol.* **85,** 182-187

53. Preiss, J., Danner, S., Summers, P. S., Morell, M., Barton, C. R., Yang, L., and Neider, M. (1990) *Plant Physiol.* **92,** 881-885

54. Okita, T. W., Nakata, P. A., Anderson, J. M., Sowokinos, J., Morell, M., and Preiss, J. (1990) *Plant Physiol.* **93,** 785-790

55. Preiss, J. (1991) in *Oxford Surveys of Plant Molecular and Cell Biology* (Miflin, B. J., ed) Vol. 7, pp. 59-114, Oxford University Press, New York

56. Krishnan, H. B., Reeves, C. D., and Okita, T. W. (1986) *Plant Physiol.* **81,** 642-645

57. Anderson, J. M., Hnilo, J., Larson, R., Okita, T. W., Morell, M., and Preiss, J. (1989) *J. Biol. Chem.* **264,** 12238-12242.

58. Plaxton, W. C., and Preiss, J. (1987) *Plant Physiol.* **83,** 105-112

59. Lin, T.-P., Caspar, T., Somerville, C., and Preiss, J. (1988) *Plant Physiol.* **86,** 1131-1135

60. Walker, J. E., Saraste, M., Runswick, M. J., and Gay, N. J. (1982) *EMBO J.* **1,** 945-951

61. Lee, Y. M., and Preiss, J. (1986) *J. Biol. Chem.* **261,** 1058-1064.

62. Lee, Y. M., Mukherjee, S., and Preiss, J. (1986) *Arch. Biochem. Biophys.* **244,** 585-595.

63. Kumar, A., Tanaka, T., Lee, Y. M., and Preiss, J. (1988) *J. Biol. Chem.* **263,** 14634-14639.

64. Parsons, T. F., and Preiss, J. (1978) *J. Biol. Chem.* **253,** 6197-6202.

65. Parsons, T. F., and Preiss, J. (1978) *J. Biol. Chem.* **253,** 7638-7645.

66. Hill, M. A., Kaufmann, K., Otero, J., and Preiss, J. (1991) *J. Biol. Chem.* **266,** 12455-12460.

67. Fu, Y., Ballicora, M. A., and Preiss, J. (1998) *Plant Physiol.* **117,** 989-996.

68. Li, L., and Preiss, J. (1992) *Carbohydr. Res.* **227,** 227-239

69. Ballicora, M. A., Laughlin, M. J., Fu, Y., Okita, T. W., Barry, G. F., and Preiss, J. (1995) *Plant Physiol.* **109,** 245-251.

70. Haugen, T., Ishaque, A., and Preiss, J. (1976) *Biochem. Biophys. Res. Commun.* **69,** 346-353.

71. Gardiol, A., and Preiss, J. (1990) *Arch. Biochem. Biophys.* **280,** 175-180.

72. Morell, M., Bloom, M., and Preiss, J. (1988) *J. Biol. Chem.* **263,** 633-637.

73. Ball, K., and Preiss, J. (1994) *J. Biol. Chem.* **269,** 24706-24711.

74. Charng, Y. Y., Iglesias, A. A., and Preiss, J. (1994) *J. Biol. Chem.* **269,** 24107-24113

75. Sheng, J., Charng, Y. Y., and Preiss, J. (1996) *Biochemistry* **35,** 3115-3121

76. Ballicora, M. A., Fu, Y., Nesbitt, N. M., and Preiss, J. (1998) *Plant Physiol.* **118,** 265-274.

77. Iglesias, A. A., Barry, G. F., Meyer, C., Bloksberg, L., Nakata, P. A., Greene, T., Laughlin, M. J., Okita, T. W., Kishore, G. M., and Preiss, J. (1993) *J. Biol. Chem.* **268,** 1081-1086.

78. Ball, K. L., and Preiss, J. (1992) *J. Protein Chem.* **11,** 231-238.

79. Iglesias, A. A., Kakefuda, G., and Preiss, J. (1992) *J. Protein Chem.* **11,** 119-128.

80. Sheng, J., and Preiss, J. (1997) *Biochemistry* **36,** 13077-13084

81. Meyer, C. R., Ghosh, P., Nadler, S., and Preiss, J. (1993) *Arch. Biochem. Biophys.* **302,** 64-71.

82. Meyer, C. R., Bork, J. A., Nadler, S., Yirsa, J., and Preiss, J. (1998) *Arch. Biochem. Biophys.* **353,** 152-159.

83. Meyer, C. R., Yirsa, J., Gott, B., and Preiss, J. (1998) *Arch. Biochem. Biophys.* **352,** 247-254.

84. Hill, M. A., and Preiss, J. (1998) *Biochem. Biophys. Res. Commun.* **244,** 573-577.

85. Monod, J., Wyman, J., and Changeaux, J. P. (1965) *J. Mol. Biol.* **12,** 88-118

86. Koshland, D. E., Jr., Nemethy, G., and Filmer, D. (1966) *Biochemistry* **5,** 365-385.

87. Wu, M. X., and Preiss, J. (1998) *Arch. Biochem. Biophys.* **358,** 182-188.

88. Wu, M. X., and Preiss, J. (2001) *Arch. Biochem. Biophys.* **389,** 159-165.

CHAPTER 2

ALTERATION OF INHIBITOR SPECIFICITY BY SITE-DIRECTED MUTAGENESIS OF ARG^{294} IN THE ADP-GLUCOSE PYROPHOSPHORYLASE FROM *ANABAENA* PCC 7120

Abstract

Phenylglyoxal modification and alanine scanning of five conserved arginine residues in the ADP-glucose pyrophosphorylase enzyme from *Anabaena* PCC 7120 indicated that residue 294 plays a specific role in inhibition by orthophosphate [Sheng, J. and Preiss, J. (1997) *Biochemistry* 36, 13077-13084]. Study of the residue was pursued by site-directed mutagenesis of Arg^{294} to lysine, glutamic acid, and glutamine. Despite the differences in charge and size, analysis of the purified mutant enzymes demonstrated similar decreases in orthophosphate affinity as was previously seen for the R294A mutant, while most of the other kinetic values were similar to those reported for the wild-type. These results suggest that the positive charge of Arg^{294} is not specifically involved in orthophosphate binding, but rather this residue is interacting with other amino acids to form the inhibitor site. Additional analysis of the mutants in the presence of different metabolic effectors indicated that the primary inhibitor for the R294A and R294Q mutants was no longer orthophosphate but rather NADPH. The R294A and R294Q mutants showed a complete reversal in the pattern of inhibitor specificity from the wild-type, with a decreased affinity for orthophosphate and an increased affinity for both NADPH and $NADP^+$.

Introduction

ADP-glucose pyrophosphorylase (ATP:α-D-glucose-1-phosphate adenylyltransferase, EC 2.7.7.27) is responsible for the first committed step in the biosynthesis of glycogen in bacteria and of starch in plants (1-4). These α-1,4-polyglucans form the major reserves of energy in their respective organisms and are necessary when carbon sources are scarce in the environment.

ADP-glucose pyrophosphorylase (ADP-Glc PPase) catalyzes the formation of ADP-glucose and pyrophosphate (PP_i) from ATP and glucose-1-P (5). ADP-Glc PPase enzymes are almost all allosterically regulated (1,6); however, there are some properties that differ between the bacterial and plant enzymes. For example, the bacterial enzymes are typically activated by glycolytic intermediates, such as fructose-1,6-bisphosphate (FBP), fructose-6-phosphate, or pyruvate, and inhibited by AMP or ADP (7). In contrast, the plant enzymes are activated by 3-phosphoglycerate (3PGA) and inhibited by orthophosphate (P_i) (2,3). The molecular size of active ADP-Glc PPases is around 200 kDa; however, the bacterial enzyme is a homotetramer (α_4) (8,9), while the plant enzyme is a heterotetramer ($\alpha_2\beta_2$) (10,11).

Cyanobacteria possess properties inherent in both plants and bacteria. The metabolic properties of cyanobacteria are more like the chloroplasts of higher-plants (12), but they synthesize glycogen as the major carbohydrate reserve similarly to bacteria (13). The ADP-Glc PPase enzymes from cyanobacteria are activated by 3PGA and inhibited by P_i like the higher-plant enzymes (14,15). The structure of cyanobacterial ADP-Glc PPase is homotetrameric like that of bacteria (15). Elucidation and subsequent

study of the deduced amino acid sequences revealed that the enzymes from cyanobacteria are more homologous to the enzymes from plants than those from bacteria (16).

Techniques such as chemical modification and site-directed mutagenesis have been used to probe the activator binding sites of ADP-Glc PPase from *Anabaena* PCC 7120. Reductive phosphopyridoxylation identified Lys^{419}, and the same treatment of the mutant K419R identified another residue, Lys^{382} (17). The activator 3PGA blocked incorporation of label at these lysyl residues, suggesting their involvement in activator binding. Subsequent mutagenesis of these residues supported the results from the chemical treatments by demonstrating decreased affinities for 3PGA (17,18). These residues are conserved in plants (16) and were also analyzed in the ADP-Glc PPases from spinach (*Spinacia oleracea*) leaf and potato (*Solanum tuberosum L.*) tuber (19-21). The results indicate that there is a conservation of functionally important residues in the activator site of ADP-Glc PPase enzymes from cyanobacteria and plants.

Further analysis of the Lys^{419} mutants that were generated for studying the activator binding site, showed that the activator specificity could be altered. Low concentrations of FBP were able to activate the K419Q mutant more effectively than 3PGA (22). This demonstrated that a change of one amino acid in the activator site of ADP-Glc PPase from *Anabaena* could affect the specificity of activation.

The identification of an inhibitor specific site in ADP-Glc PPase from *Anabaena* followed similar methodology as for the activator binding sites. A combination of phenylglyoxal treatment and mutagenesis of five highly conserved arginine residues to alanines showed the importance of arginine at position 294, as the apparent affinity for the inhibitor P_i decreased significantly (23). This arginine is conserved throughout

cyanobacterial and plant enzymes. Further analysis was necessary to understand the role arginine plays in inhibition since both cyanobacteria and plant ADP-Glc PPases share inhibition by P_i. In this work, we determined the importance of size and charge in P_i inhibition at position Arg^{294} by utilizing the methodology of site-directed mutagenesis, replacing the arginine with lysine, glutamic acid, or glutamine. Also, we show for the first time a change in the inhibitor specificity by mutation of an ADP-Glc PPase enzyme.

Site-Directed Mutagenesis. Site-directed mutagenesis was performed using the QuikChange™ Site-Directed Mutagenesis Kit from Stratagene. The plasmid pAraE3a was utilized for both mutagenesis and expression (17,18,24). The mutations at position 294 were designated as R294K, R294E, and R294Q. These mutants were created utilizing the following oligonucleotides:

R294K 5' - TTATACCCGCGCTAAGTACTTACCACCCA - 3'

R294E 5' - TTATACCCGCGCTGAGTACTTACCACCCA - 3'

R294Q 5' - TTATACCCGCGCTCAGTACTTACCACCCA - 3'

The coding regions of the mutated plasmids were sequenced by dideoxy sequencing (25) to ensure that no unintended mutations were introduced.

Expression and Purification of Mutant Enzymes. The mutant enzymes were expressed in the *Escherichia coli* (*E. coli*) bacterial strain AC70R1-504 that is deficient in

Materials and Methods

Materials. [^{14}C]Glucose-1-P was obtained from ICN Pharmaceuticals Inc. [^{32}P]PP_i was purchased from NEN Life Science Products. Perfect™ protein markers were purchased from Novagen, Inc. Oligonucleotides were synthesized and purified by the Macromolecular Facility at Michigan State University. All other reagents were purchased at the highest quality available.

Site-Directed Mutagenesis. Site-directed mutagenesis was performed using the QuikChange™ Site-Directed Mutagenesis Kit from Stratagene. The plasmid pAnaE3a was utilized for both mutagenesis and expression (17,18,24). The mutations at position 294 were designated as R294K, R294E, and R294Q. These mutants were created utilizing the following oligonucleotides:

R294K 5' - TTATACCCGCGCT**AAG**TACTTACCACCCA - 3'

R294E 5' - TTATACCCGCGCT**GAG**TACTTACCACCCA - 3'

R294Q 5' - TTATACCCGCGCT**CAG**TACTTACCACCCA - 3'

The coding regions of the mutated plasmids were sequenced by dideoxy sequencing (25) to ensure that no unintended mutations were introduced.

Expression and Purification of Mutant Enzymes. The mutant enzymes were expressed in the *Escherichia coli* (*E. coli*) bacterial strain AC70R1-504 that is deficient in

endogenous ADP-Glc PPase activity. The mutant enzymes were purified as previously described for the subcloned wild-type enzyme and the R294A mutant enzyme (23).

Enzyme Assay. Assay A) Pyrophosphorolysis. [^{32}P]ATP formation at 37 °C was measured by the method of Preiss *et al.* (7). The reaction mixtures consisted of 80 mM HEPES buffer (pH 7.0), 8 mM $MgCl_2$, 1.5 mM [^{32}P]PP_i (300 to 1000 cpm/nmol), 2 mM ADP-glucose, 4 mM NaF, 4 mM 3PGA, and 0.05 mg/mL bovine serum albumin (BSA), plus enzyme in a total volume of 250 μL.

Assay B) Synthesis. [^{14}C]ADP-glucose formation at 37 °C was measured by the method of Preiss *et al.* (7). The reaction mixtures contained 100 mM HEPES buffer (pH 8.0), 7 mM $MgCl_2$, 0.5 mM [^{14}C]Glc-1-P (~1000 cpm/nmol), 1.5 mM ATP, 0.0015 U/μL pyrophosphatase, and 0.2 mg/mL BSA, plus enzyme in a total volume of 200 μL. For activated conditions the mixture contained 0.5 mM 3PGA, except for R294E, which contained 8 mM 3PGA to measure the inhibition by P_i.

In the above assays, one unit of enzyme activity is equal to 1 μmol of product, either [^{32}P]ATP or [^{14}C]ADP-glucose, formed per minute at 37 °C .

Kinetic Characterization. Kinetic data were plotted as initial velocity versus substrate or effector concentration. Kinetic constants were determined by fitting of the data with a non-linear least square fit and with the Hill equation using the program Origin™ 5.0. n_H, the Hill coefficient, and $A_{0.5}$, $S_{0.5}$, and $I_{0.5}$, the kinetic constants that correspond to the concentration of activator, substrate, or inhibitor giving 50% of the maximal activation, velocity, or inhibition, respectively, were calculated from Hill plots.

Protein Assay. Enzyme concentration was determined by using bicinchoninic acid reagent (26) from Pierce Chemical Company, with BSA as the standard.

Protein Electrophoresis and Immunoblotting. SDS-PAGE was done according to Laemmli (27), using 4-15% Tris-HCl pre-cast gradient polyacrylamide gels from Bio-Rad. Molecular weight markers were Perfect^{TM} protein markers. After electrophoresis, proteins were visualized by staining with Coomassie Brilliant Blue R-250 or electroblotted onto a Protran^{TM} (Schleicher & Schuell) nitrocellulose membrane. The nitrocellulose membrane was then treated with affinity-purified anti-spinach leaf ADP-Glc PPase IgG, and the antigen-antibody complex was visualized via treatment with alkaline phosphatase-linked goat anti-rabbit IgG and subsequent staining by BM purple AP-substrate precipitating reagent (15).

Results

Expression and Purification of the Mutant Enzymes. The expression of the Arg^{294} mutant enzymes was analyzed by SDS-PAGE of the crude extract proteins, then by immunoblotting with anti-spinach leaf ADP-glucose PPase IgG, which was previously shown to react with the enzyme from *Anabaena* (15). Compared to a control with the wild-type enzyme, the expression of these mutant enzymes was similar, as were the molecular sizes (data not shown). The purification of the mutant enzymes closely resembled the purification of R294A (23), and the mutants were purified to greater than 90% purity as determined by SDS-PAGE (data not shown). These purified enzymes were then used for the following analyses.

Kinetic Characterization of the Mutant Enzymes. The mutant enzymes were analyzed in the synthesis direction (assay B) to compare the kinetic parameters with the values previously reported for the wild-type and R294A mutant enzyme (23). The $S_{0.5}$ values for the substrates, ATP, $MgCl_2$, and Glc-1-P, for the mutant enzymes were similar to those of the wild-type ADP-Glc PPase enzyme (Table I). This suggested that the conformation of the active site was not affected. The $S_{0.5}$ values for ATP of the mutants were increased only 2- to 4-fold over wild-type, and the $S_{0.5}$ values for Mg^{2+} were slightly less than 2-fold different (Table I). The most striking difference, between mutant R294E and wild-type, was the 16-fold increase in $A_{0.5}$ for 3PGA, from 0.050 to 0.8 mM (Table I).

The P_i inhibition patterns of the R294K, R294E, and R294Q mutants under non-activated conditions differed from those of the wild-type (Figure 1A), as the mutants could only be inhibited to 50-60% initial activity up to 10 mM P_i. As seen previously,

Table I. Kinetic parameters of the *Anabaena* wild-type and Arg^{294} mutant enzymes[a]

	ATP		Glc-1-P		Mg^{2+}		3PGA	
	$S_{0.5}$ (mM)	n_H	$S_{0.5}$ (mM)	n_H	$S_{0.5}$ (mM)	n_H	$A_{0.5}$ (mM)	n_H
wild-type[b]	0.11 ± 0.01	1.2	0.034 ± 0.004	0.9	3.0 ± 0.3	4.2	0.050 ± 0.005	1.0
R294A[b]	0.13 ± 0.01	1.3	0.022 ± 0.001	1.0	3.4 ± 0.1	4.7	0.030 ± 0.001	1.6
R294K	0.33 ± 0.02	1.3	0.04 ± 0.01	0.9	1.7 ± 0.1	3.2	0.020 ± 0.004	1.3
R294Q	0.21 ± 0.03	1.3	0.03 ± 0.01	0.8	1.45 ± 0.04	3.9	0.041 ± 0.006	1.5
R294E	0.40 ± 0.04	2.1	0.05 ± 0.02	1.1	2.0 ± 0.1	3.3	0.8 ± 0.2	1.1

[a] Reactions were performed using assay B under activated conditions as described in the "Materials and Methods." Data is an average of at least two experiments with the difference expressed as a ± deviation.

[b] Values are obtained from (23).

Figure 1. Inhibition of *Anabaena* wild-type (■) and R294K (□), R294E (○), and R294Q (Δ) mutant enzymes by orthophosphate in the absence (A) and in the presence of 3PGA (B). Reactions were performed in the synthesis direction as indicated in Materials and Methods. For (A), 100% activity was 1.4, 4.0, 1.3, and 0.76 nmol of ADP-glucose formed per 10 min for wild-type, R294K, R294E, and R294Q, respectively. For (B), which includes the R294A (∇) mutant, 100% activity was 3.8, 4.0, 1.2, 3.0, and 2.1 nmol of ADP-glucose formed per 10 min for wild-type, R294A, R294K, R294E, and R294Q, respectively. In the presence of 3PGA (B), the same level of saturation (10 x $A_{0.5}$) was obtained at 0.5 mM for the wild-type, R294A, R294K, and R294Q, and at 8 mM for R294E. The data represent an average of separate experiments.

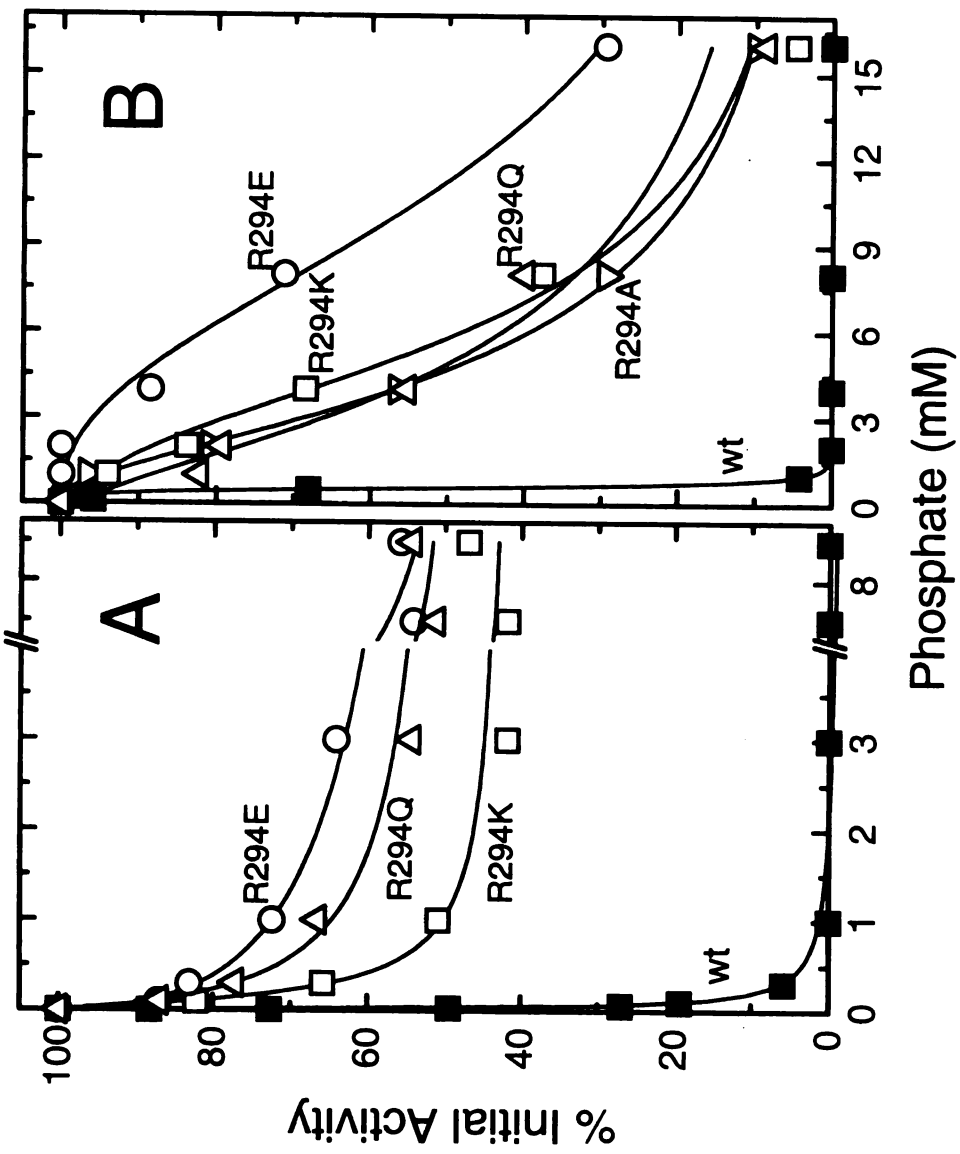
A
B
% Initial Activity
Phosphate (mM)
R294E
R294Q
R294K
R294A
wt
0
20
40
60
80
100
0
1
2
3
8
0
3
6
9
12
15

Figure 1.

the wild-type *Anabaena* enzyme was almost completely inhibited by 1 mM P_i. Though not shown, the R294A enzyme exhibited a similar inhibition pattern to the other mutants, reaching a comparable maximal inhibition level by 10 mM P_i (23).

The R294 mutants again showed different P_i inhibition patterns compared to the wild-type under activated conditions (Figure 1B), with at least a 10-fold shift in $I_{0.5}$ for P_i over wild-type. The R294A, R294K, and R294Q mutants showed less than 20% activity at 16 mM P_i, a level reached by 1 mM for the wild-type. The 3PGA concentration for wild-type, R294A, R294K, and R294Q was 0.5 mM, a level used to saturate the enzymes (10 x $A_{0.5}$). R294E at 0.5 mM 3PGA would not be fully activated at this concentration (Table I) and consequently shows a similar inhibition pattern to the wild-type (data not shown). The R294E mutant in saturating conditions of 3PGA (8 mM) showed a much different curve compared to wild-type, shifting almost 25-fold over wild-type at 50% inhibition (Figure 1B).

The specific activities of the Arg^{294} mutant enzymes were analyzed from purified extracts. The R294Q enzyme exhibited comparable V_{max} values to the wild-type enzyme under both non-activated and activated conditions (Table II). In the presence of the activator 3PGA, the R294K enzyme showed a slightly lowered (1.4-fold) value for the V_{max} compared to the wild-type; however, in the absence of activator R294K was 2.4-fold higher in V_{max} than the wild-type. The R294E mutant enzyme exhibited lowered V_{max} values compared to the wild-type in both non-activated and activated conditions, 5- and 3-fold, respectively.

Effector Specificity of the Mutant Enzymes. Since mutagenesis of the activator site can lead to a modification of the specificity for the activator (22), we studied the

Table II. Comparison of specific activities of the *Anabaena* wild-type and Arg^{294} mutant enzymes[a]

	3PGA	wild-type	R294K	R294Q	R294E
V_{max} (U/mg)	-	6.3	15	7.2	1.2
	+	127	90	119	44

[a] Reactions were performed in the synthesis direction, assay B as described under "Materials and Methods." The data represent the mean of two separate experiments, and the differences were less than 5% error. Values were in good agreement with the V_{max} obtained in the saturated region of the substrate curve (Table I).

specificity of regulation of these inhibitor mutants. The mutants were assayed in the presence of some of the major activators and inhibitors of other bacterial enzymes (11). The most notable change in effector specificity was for the R294A and R294Q enzymes, as 2 mM NADPH was able to inhibit these mutants by greater than 90%, while 2 mM P_i inhibited them by only 20% (Table III). This is in contrast to the inhibitor specificity of the wild-type, which is inhibited 90% by 2 mM P_i and only 30% by 2 mM NADPH. Indeed, the NADPH inhibition pattern of the R294A and R294Q enzymes indicates a change in specificity, as these mutants showed a decrease in $I_{0.5}$ for NADPH of 10- and 2-fold compared to the wild-type, in the absence and presence of 3PGA, respectively (Figure 2, A and B). The R294K mutant enzyme was also inhibited 90% at 2 mM NADPH, but it showed 50% inhibition at 2 mM P_i. The R294E enzyme exhibited 60% and 40% inhibition at 2 mM NADPH and P_i, respectively.

The mutant enzymes in the presence of the other compounds showed similar results to the wild-type, except for P-enolpyruvate and FBP (Table III). P-enolpyruvate at a concentration of 5 mM activated the R294 mutants 7- to 19-fold but only 2-fold for the wild-type; however, 3PGA remained the major activator for all the mutants (Table III). In the presence of 5 mM FBP, the R294A and R294Q mutants exhibited inhibition by FBP, whereas the wild-type, R294K, and R294E enzymes were activated (Table III).

To determine if the inhibition of the R294A and R294Q enzymes was specific for NADPH or subject to other phosphopyridine nucleotides, the mutants were assayed in the presence of NAD^+, NADH, $NADP^+$, or NADPH. NADPH was still the major inhibitor for the R294A and R294Q enzymes, but $NADP^+$ was able to inhibit these

Table III. Specificity of allosteric effectors of the *Anabaena* wild-type and Arg^{294} mutant enzymes[a]

Effectors	mM	wild-type	R294K	R294A	R294Q	R294E
		ADP-glucose formed (nmol/10 min)				
None		2.97	0.95	3.27	3.46	1.57
		Relative Activity				
None		1.0	1.0	1.0	1.0	1.0
Fructose-6-P	5	9.9	6.1	17.5	12.9	17.4
Fructose-1,6-P_2	5	3.1	2.8	0.4	0.5	1.2
Glucose-6-P	5	7.8	7.2	16.8	12.9	7.6
Glucose-1,6- P_2	5	0.4	0.3	0.1	0.1	0.7
P-enolpyruvate	5	2.4	7.8	19.2	14.1	7.2
Pyruvate	5	1.4	0.8	0.9	0.9	1.6
2,3-P-glycerate	5	0.2	0.2	0.3	0.3	0.9
3PGA	5	17.1	9.8	24.6	19.9	23.8
NADPH	2	0.7	0.1	<0.1	0.1	0.4
ADP	2	1.3	0.7	1.0	1.0	1.3
AMP	2	2.8	1.1	3.9	3.2	6.3
P_i	2	0.1	0.5	0.8	0.8	0.6

[a] Reactions were performed using assay B as described under "Materials and Methods" with the presence of effectors as indicated.

Figure 2. Inhibition of Anabaena wild-type (■) and R294A (▽) and R294Q (Δ) mutant enzymes by NADPH in the absence (A) and in the presence of 3PGA (B). Reactions were performed in the synthesis direction as indicated in Materials and Methods. For (A), 100% activity was 2.2, 2.4, and 2.4 nmol of ADP-glucose formed per 10 min for wild-type, R294A, and R294Q, respectively. For (B), 100% activity was 14.0, 10.7, and 11.1 nmol of ADP-glucose formed per 10 min for wild-type, R294A, and R294Q, respectively. The data represent an average of separate experiments.

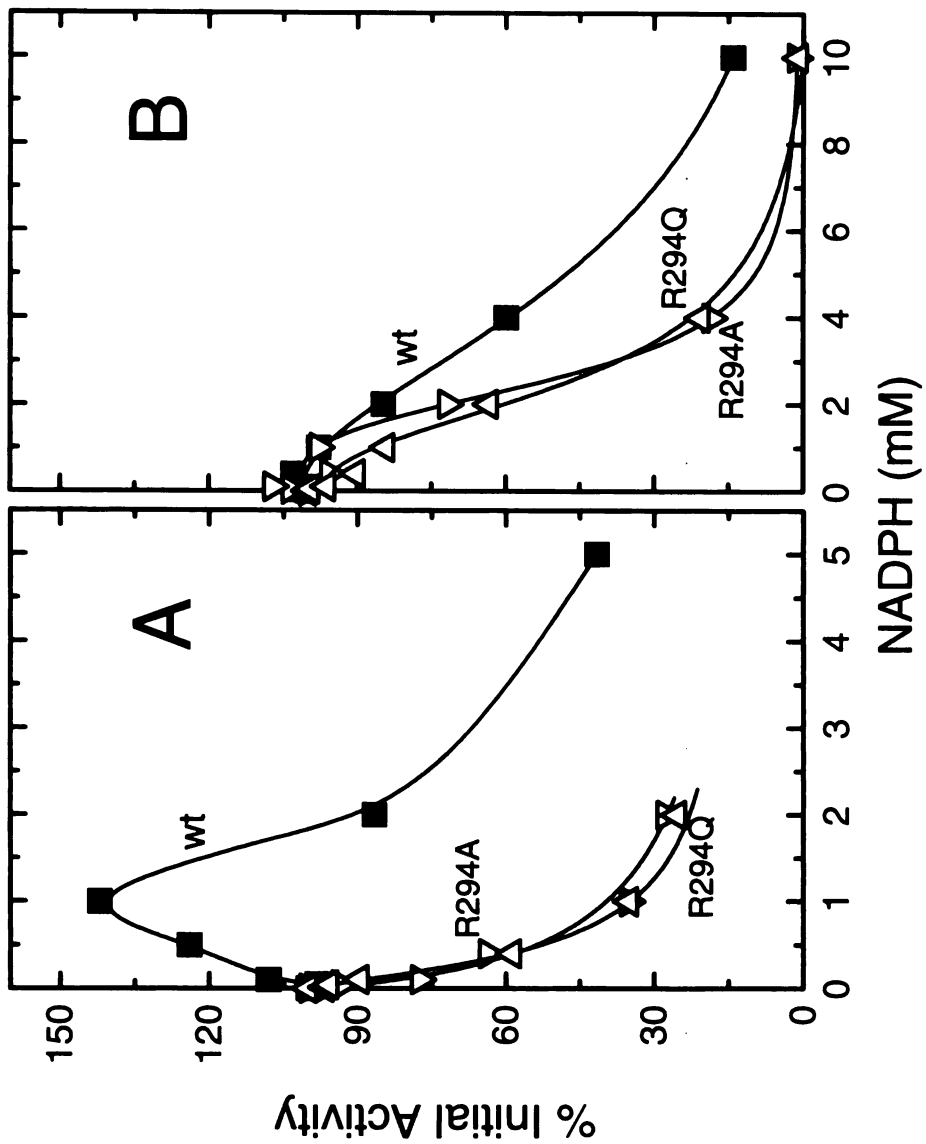
A
B
wt
R294A
R294Q
% Initial Activity
NADPH (mM)
0
30
60
90
120
150
0
1
2
3
4
5
6
8
10

Figure 2.

mutants by 60% (Table IV). The two diphosphopyridine nucleotides did not affect the activity of the R294A and R294Q mutants.

Table IV. Effect of different phosphopyridine nucleotides on the *Anabaena* wild-type and R294A and R294Q mutant enzymes[a]

Effectors	mM	wild-type	R294A	R294Q
		ADP-Glucose formed nmol/10 min		
None		1.95	1.76	1.71
		Relative Activity		
None		1.00	1.00	1.00
NAD^+	2	1.17	1.27	1.23
NADH	2	1.11	0.97	0.89
$NADP^+$	2	1.49	0.43	0.43
NADPH	2	0.91	0.06	0.07

[a] Reactions were performed in the synthesis direction, assay B as described under "Materials and Methods."

Discussion

The results of this study show that mutation of Arg^{294} in ADP-Glc PPase from *Anabaena* to another residue causes a decrease in sensitivity to the inhibitor P_i, regardless of the charge and size of the substituted residue. However, depending on the type of residue substituted, Lys, Glu, Gln, or even Ala (23), the mutation can affect more than P_i sensitivity, even altering the inhibitor specificity of some of the mutant enzymes.

In absence of the activator 3PGA, all of the mutants showed a marked decrease in P_i sensitivity (Figure 1A). R294E and R294Q were less sensitive than R294K, yet the maximum inhibition reached by any of these mutants up to 10 mM P_i was still at least 50% of the initial activity. This effect was seen previously (23), and any further inhibition at even higher concentrations of P_i was attributed to the ionic strength of the solution. The current study saw a similar pattern of inhibition to the R294A mutant under non-activated conditions at P_i concentrations below 10 mM.

In presence of the activator, the Arg^{294} mutants demonstrated two major shifts of the inhibition curve from the wild-type (Figure 1B). The first shift corresponds to the activated mutants R294A, R294K, and R294Q. The non-polar, basic, and polar substitutions, respectively, all cause a similar shift that most probably results from size differences at the site compared to the arginine of the wild-type. The second shift belongs to the activated R294E mutant, and though it is also different in size, it possesses a negative charge, opposite from the wild-type. The data in this curve show that neither the charge nor the size of Arg^{294} is the lone component of the P_i interaction occurring at this site. If a positive charge was the major contributor, one would expect the conserved change from arginine to lysine to produce the smallest difference between inhibitor

affinities among the mutants. However, as lysine and arginine share a conserved charge, they do not share similar molecular dimensions, so other factors must contribute to the phosphate sensitivity seen at position 294. Charge might still have some effect on the affinity for P_i since the substitution from arginine to glutamic acid (opposite charge) produced an enzyme that is least sensitive to P_i inhibition. However, this mutant can still be partially inhibited between 6-12 mM P_i (Figure 1B).

Other parameters of R294E were altered, such as the V_{max} and the affinity for the activator, 3PGA. The V_{max} decreased slightly, 5- and 3-fold in non-activated and activated conditions, respectively (Table II), and the $A_{0.5}$ for 3PGA increased 16-fold (Table I). The change in the V_{max} can be attributed to a disruption of the local environment of the active site. It is possible that the negative charge introduced by mutagenesis mimics the presence of the inhibitor P_i. This is in agreement with the fact that this R294E mutant had a low specific activity in absence of activator (Table II), as if the enzyme was already in a slightly inhibited state. In presence of saturating concentrations of the activator, the activity of R294E increases but does not reach the same level as the wild-type (Table II). In allosteric enzymes it has been observed that the binding of one effector can cause a change in the binding affinity of other subsequent effectors (28). In the study of activator/inhibitor binding for ADP-Glc PPases from *Anabaena*, it was shown that the binding of activator, 3PGA, causes a decrease in the apparent affinity of the enzyme for the inhibitor P_i (15,17,24). In this mutant, R294E, the negative charge of the glutamic acid probably mimics the presence of a weak but permanent inhibitor that hinders the activator from re-establishing the conformation for maximal activity. The glutamic acid might not cause a big increase in inhibition but may

cause the decreased affinity for the activator due to the residual presence of the negative charge.

An interesting result from the analysis of different effectors with these Arg^{294} mutants is the change in inhibitor specificity for the R294A, R294Q, and even the R294K mutants. These mutants were inhibited at least 90% by 2 mM NADPH (Table III), while the major inhibitor for wild-type ADP-Glc PPases from cyanobacteria is P_i (14,15). This specificity of inhibition included only triphosphopyridine nucleotide compounds (Table IV), suggesting the importance of the extra phosphate in this interaction. R294A and R294Q were even inhibited by FBP (Table III), which could be considered as an analog of part of NADPH because FBP shares a ribose-bis-P structure. The switch in inhibitor specificity suggests that there has been a conformational change of the inhibitor site of these mutants that prefers ribose-P binding to P_i. These results also suggest that residue 294 is not the inhibitor binding site per se, rather it interacts with other amino acid residues to form the inhibitor binding site. This variation in specificity is found more commonly for the activators of various ADP-Glc PPases, where a class of the enzyme will have primary and secondary activators (29). For the activator sites the variation suggests a similarity between classes, and thus a mutation of part of the gene specifying the activator site can allow adaptation of the activator specificity to coordinate with the metabolic activities of the organism. Even though the different classes of ADP-Glc PPases have only one primary inhibitor, they include AMP, ADP, and P_i (29). Thus it would be reasonable to hypothesize that the same adaptability of the inhibitor site would be possible, allowing a mutation of the inhibitor, i.e. R294A or R294Q, to change

the specificity of inhibition. This suggests that the differences in inhibition could have occurred by divergence of the inhibitor site in the evolution of these enzymes.

ADP-glucose pyrophosphorylases from different sources catalyze the same reaction, but are subject to control through various metabolites unique to the carbon assimilation pathway of the organism (30). As kinetic characterization of many of the ADP-Glc PPase enzymes has been done, it is of interest to understand the molecular interactions between the ligands and the protein surfaces. A 3-D structure of a member of the ADP-Glc PPase family will be helpful in this endeavor, and work is currently in progress to answer this and other questions remaining about ADP-Glc PPase.

References

1. Preiss, J. (1984) *Annu. Rev. Microbiol.* **38,** 419-458
2. Preiss, J., and Sivak, M. N. (1998) in *Comprehensive Natural Products Chemistry* (Pinto, B. M., ed) Vol. 3, pp. 441-495, Pergamon Press, Oxford
3. Ghosh, H. P., and Preiss, J. (1966) *J. Biol. Chem.* **241,** 4491-4504
4. Preiss, J. (1991) in *The Biochemistry of Plants* (Preiss, J., ed) Vol. 14, pp. 184-249, Academic Press, San Diego
5. Espada, J. (1962) *J. Biol. Chem.* **237,** 3577-3581
6. Preiss, J. (1982) *Annu. Rev. Plant Physiol.* **33,** 432-454
7. Preiss, J., Shen, L., Greenberg, E., and Gentner, N. (1966) *Biochemistry* **5,** 1833-1845
8. Ozaki, H., and Preiss, J. (1972) *Methods Enzymol.* **28,** 406-413
9. Haugen, T. H., Ishaque, A., and Preiss, J. (1976) *J. Biol. Chem.* **251,** 7880-7885
10. Morell, M. K., Bloom, M., Knowles, V., and Preiss, J. (1987) *Plant Physiol.* **85,** 182-187
11. Preiss, J. (1991) in *Oxford Surveys of Plant Molecular and Cell Biology* (Mifflin, B., ed) Vol. 7, pp. 59-114, Oxford University Press, Oxford
12. Aitken, A. (1988) *Methods Enzymol.* **167,** 145-154
13. Shively, J. M. (1988) *Methods Enzymol.* **167,** 195-203
14. Levi, C., and Preiss, J. (1976) *Plant Physiol.* **58,** 753-756
15. Iglesias, A. A., Kakefuda, G., and Preiss, J. (1991) *Plant Physiol.* **97,** 1187-1195
16. Smith-White, B. J., and Preiss, J. (1992) *J. Mol. Evol.* **34,** 449-464

17. Charng, Y. Y., Iglesias, A. A., and Preiss, J. (1994) *J. Biol. Chem.* **269,** 24107-24113

18. Sheng, J., Charng, Y. Y., and Preiss, J. (1996) *Biochemistry* **35,** 3115-3121

19. Morell, M., Bloom, M., and Preiss, J. (1988) *J. Biol. Chem.* **263,** 633-637.

20. Ball, K., and Preiss, J. (1994) *J. Biol. Chem.* **269,** 24706-24711.

21. Ballicora, M. A., Fu, Y., Nesbitt, N. M., and Preiss, J. (1998) *Plant Physiol.* **118,** 265-274.

22. Charng, Y. Y., Sheng, J., and Preiss, J. (1995) *Arch. Biochem. Biophys.* **318,** 476-480

23. Sheng, J., and Preiss, J. (1997) *Biochemistry* **36,** 13077-13084

24. Charng, Y. Y., Kakefuda, G., Iglesias, A. A., Buikema, W. J., and Preiss, J. (1992) *Plant Mol. Biol.* **20,** 37-47

25. Sanger, F., Nicklen, S., and Coulson, A. R. (1977) *Proc. Natl. Acad. Sci. U. S. A.* **74,** 5463-5467

26. Smith, P. K., Krohn, R. I., Hermanson, G. T., Mallia, A. K., Gartner, F. H., Provenzano, M. D., Fujimoto, E. K., Goeke, N. M., Olson, B. J., and Klenk, D. C. (1985) *Anal. Biochem.* **150,** 76-85

27. Laemmli, U. K. (1970) *Nature* **227,** 680-685

28. Monod, J., Changeux, J., and Jacob, F. (1963) *J. Mol. Biol.* **6,** 306-329

29. Preiss, J. (1973) in *The Enzymes* (Boyer, P. D., ed) Vol. 8, pp. 73-119, Academic Press, New York

30. Sivak, M. N., and Preiss, J. (1998) in *Advances In Food and Nutrition Research* (Taylor, S. L., ed) Vol. 41, pp. 1-199, Academic Press, San Diego

CHAPTER 3

ASPARTATE RESIDUE 142 IS IMPORTANT FOR CATALYSIS BY ADP-GLUCOSE PYROPHOSPHORYLASE FROM *ESCHERICHIA COLI*

Frueauf, J. B., Ballicora, M. A., and Preiss, J. (Aug. 2001) have submitted the data in this chapter for publication in the Journal of Biological Chemistry.

Abstract

Structural prediction of several bacterial and plant ADP-glucose pyrophosphorylases, as well as of other sugar-nucleotide pyrophosphorylases, was used for comparison with the 3-D structures of two crystallized pyrophosphorylases (Brown *et al.* (1999) EMBO J. 18, 4096-4107 and Blankenfeldt *et al.* (2000) EMBO J. 19, 6652-6663). This comparison led to the discovery of highly conserved residues throughout the super-family of pyrophosphorylases despite the low overall homology. One of those residues, Asp^{142} in the ADP-glucose pyrophosphorylase from *Escherichia coli*, was predicted to be near the substrate site. To elucidate the function that Asp^{142} might play in the *Escherichia coli* ADP-glucose pyrophosphorylase, aspartate was replaced by alanine, asparagine, or glutamate using site-directed mutagenesis. Kinetic analysis in the direction of synthesis or pyrophosphorolysis of the purified mutants showed a decrease in specific activity of up to 4 orders of magnitude. Comparison of other kinetic parameters, i.e. the apparent affinities for substrates and allosteric effectors, showed no significant changes, excluding this residue from the specific role of ligand binding. Only the D142E mutant exhibited altered K_m values but none as pronounced as the decrease in specific activity. These results show that residue Asp^{142} is important in the catalysis of the ADP-glucose pyrophosphorylase from *Escherichia coli*.

Introduction

Glycogen and starch, which consist of mainly α-1,4-polyglucans, encompass most of the energy reserves in organisms. The biosynthesis of these polysaccharides proceeds from the formation of the glucosyl donor, ADP-glucose (ADP-Glc). ADP-glucose pyrophosphorylase (ADP-Glc PPase, EC 2.7.7.27) catalyzes the synthesis of ADP-Glc and pyrophosphate (PP_i) from ATP and glucose-1-phosphate (Glc-1-P) (1). This reversible reaction is the key regulatory step in the production of glycogen in bacteria and of starch in plants (2-5).

ADP-Glc PPase has been isolated and characterized from various sources. Most of the enzymes are allosterically regulated by the glycolytic intermediates of the major pathway of carbon assimilation in the organism (6). The regulatory effectors include the activator fructose-1,6-bisphosphate (FBP) and the inhibitor AMP for an enzyme from enteric bacteria, e.g. *Escherichia coli* (7), and the activator 3-phosphoglycerate (3PGA) and the inhibitor orthophosphate for enzymes from plants and other photosynthetic organisms, e.g., algae and cyanobacteria (4,5). Active ADP-Glc PPase forms a tetramer of about 200 kDa, which is either homomeric (α_4) in bacteria (8,9) or heteromeric ($\alpha_2\beta_2$) in plants (10,11). The emergence of two different subunits in plants, designated as small and large based on disparities in molecular weight, likely arose from the need for tissue-specific regulation (5,12). Also, other studies show that each subunit has a separate function: the small subunit is catalytic while the large subunit is a mediator of the allosteric regulation of the small subunit (13).

The 3-D structure of an ADP-Glc PPase has not yet been resolved by X-ray crystallography; however, many structural studies have been performed using other

approaches. A combination of techniques, such as chemical modification and site-directed mutagenesis, has been applied to study the ADP-Glc PPase enzyme from *E. coli*. Azido-based photoaffinity analogs of the ATP substrate and the ADP-Glc substrate (pyrophosphorolysis direction) were used to probe the substrate-binding site. Analysis of the covalently labeled enzyme revealed Tyr^{114} as the modified residue, and subsequent site-directed mutagenesis of the residue showed a marked decrease in affinity for ATP, as well as a decrease in affinity for Glc-1-P and for FBP (14). The residue likely interacts with the adenine ring of ATP but is not crucial for the binding of the substrate. Pyridoxal-5-phosphate (PLP), a mild reagent that modifies lysines within ligand binding sites upon reduction by $NaBH_4$, is an analog of the activator from *E. coli*, FBP. Reaction of this modifying agent with the enzyme labels two different lysines, Lys^{39} and Lys^{195} that are blocked by the inclusion of FBP and of the substrate ADP-Glc, respectively (15,16). Mutation of Lys^{39} showed this residue is important in the interaction of the activator FBP with the enzyme (17). Mutagenesis of the Lys^{195} residue produced enzymes with drastically increased K_m values for Glc-1-P, while the other kinetic constants and the k_{cat} were not altered, showing clearly that this residue is involved in the binding of Glc-1-P in both bacterial and plant enzymes (18,19).

These techniques have also been used to probe the regulatory sites of ADP-Glc PPases from photosynthetic organisms. Studies of PLP modified residues in the ADP-Glc PPases from spinach (*Spinacia oleracea*) leaves and the cyanobacterium *Anabaena* PCC 7120 have implicated specific lysine residues located in the C-terminus that are involved in the binding of the activator 3PGA (20-22). These residues are not present in the bacterial enzymes. Site-directed mutagenesis of these homologous residues

in ADP-Glc PPase from *Anabaena* and from the heterotetrameric enzyme from potato (*Solanum tuberosum* L.) tuber specifically affects the apparent affinity for activator (22,23). The results from the above structural studies show that functionally important residues located in the active site are conserved in ADP-Glc PPases from different organisms; however, the residues related to the regulation of these enzymes seem to have diverged.

Protein sequence alignments of ADP-Glc PPases show a high degree of conservation (85-95% similarity) among enzymes from bacteria and among the small subunits of plants; however, the similarity between the two groups is about half (30-40%) (24). Inclusion of the large subunits from plants in the alignment with the small subunits improves the percent similarity slightly (50-60%) from the comparison between bacteria and the small subunits. The degree of similarity can be increased for enzymes from bacteria and the small and large subunits when limiting the comparison to the region containing roughly the first 200 residues (Figure 1). Within this region, many residues are highly conserved among the various ADP-Glc PPases. Moreover, the region contains at least a few key residues conserved throughout other enzymes that catalyze the synthesis of a nucleoside diphosphate sugar from a sugar-phosphate and a nucleoside triphosphate (19). Although these enzymes have been characterized thoroughly by the above methods, a residue involved in the catalytic reaction has not been isolated. The 3-D structure of an ADP-Glc PPase will likely be of help in this endeavor, and work on the crystallography is in progress. In the meantime, a prediction of the structure of ADP-Glc PPase is needed to interpret the relationship between the available genetic and

Figure 1. Prediction of the secondary structure of several ADP-Glc PPases. The ADP-Glc PPase sequences predicted were from *Escherichia coli* (ecoli), *Bacillus stearothermophilus* (bst_c), *Anabaena* PCC 7120 (anaba), *Solanum tuberosum* L. small subunit (stuss), *Agrobacterium tumefaciens* (agrob), and *Rhodobacter sphaeroides* (r_sph) and were aligned with *N*-acetylglucosamine 1-phosphate uridyltransferase (GlmU) and dTDP-glucose pyrophosphorylase (RmlA). The secondary structure of each ADP-Glc PPase was predicted as indicated in "Experimental Procedures." Residues in blue and light blue were predicted as a β-sheet with a high or low level of confidence, respectively. Red and pink were predicted as an α-helix with a high or low level of confidence, respectively. Green colored residues in the prediction were indicated as neither α-helix nor β-sheet (loops). In black are residues that the PHD program could not make a prediction. For GlmU and RmlA, the colors indicate the known secondary structure based on the solved crystal structure (25,26). Insertions and deletions were introduced to maximize the alignment of both primary and secondary structure. Asterisks indicate residues that are conserved between the consensus of the ADP-Glc PPases analyzed and GlmU and RmlA, respectively. Residues K39, Y114, and K195 are the amino acids in the ADP-Glc PPase from *E. coli* that interact with the activator FBP, and the substrates ATP and Glc-1-P, respectively. Regions 1, 2, and 3 form the putative catalytic domain. Region 1 could also interact with the regulatory domain. Region 4 is also predicted as part of the catalytic domain from the comparison with the 3-D structures of GlmU and RmlA. White triangles indicate residues where proteinase K cuts in the *E. coli* enzyme (48). Black triangles indicate where the ADP-Glc PPase from *Anabaena* is cut by trypsin under conditions of partial proteolysis (Charng, Y. and J. Preiss, unpublished results). Gray triangles indicate where trypsin cuts the *E. coli* enzyme (Wu, M. and J. Preiss, unpublished results). The yellow arrow shows the position of the amino acid Asp^{142} that was mutated. Images in this thesis are presented in color.

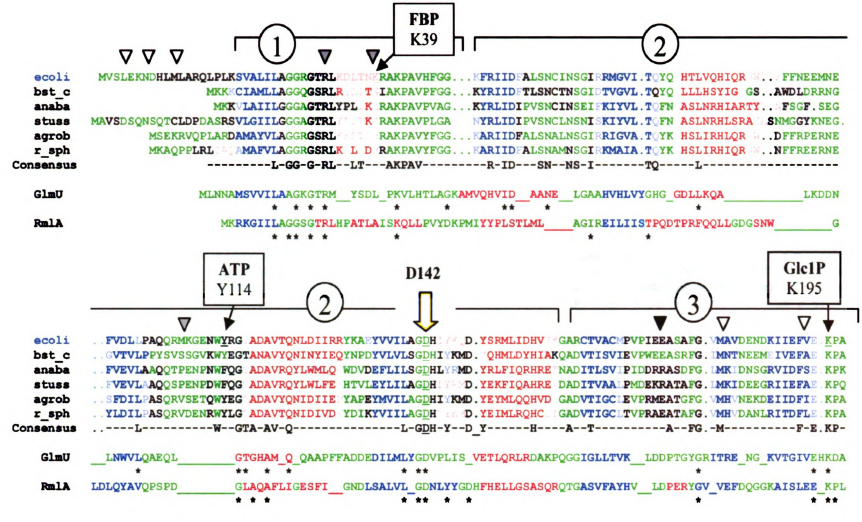
FBP
K39
1
2
ecoli
bst_c
anaba
stuss
agrob
r_sph
Consensus
GlmU
RmlA
ATP
Y114
D142
Glc1P
K195
3

Figure 1.

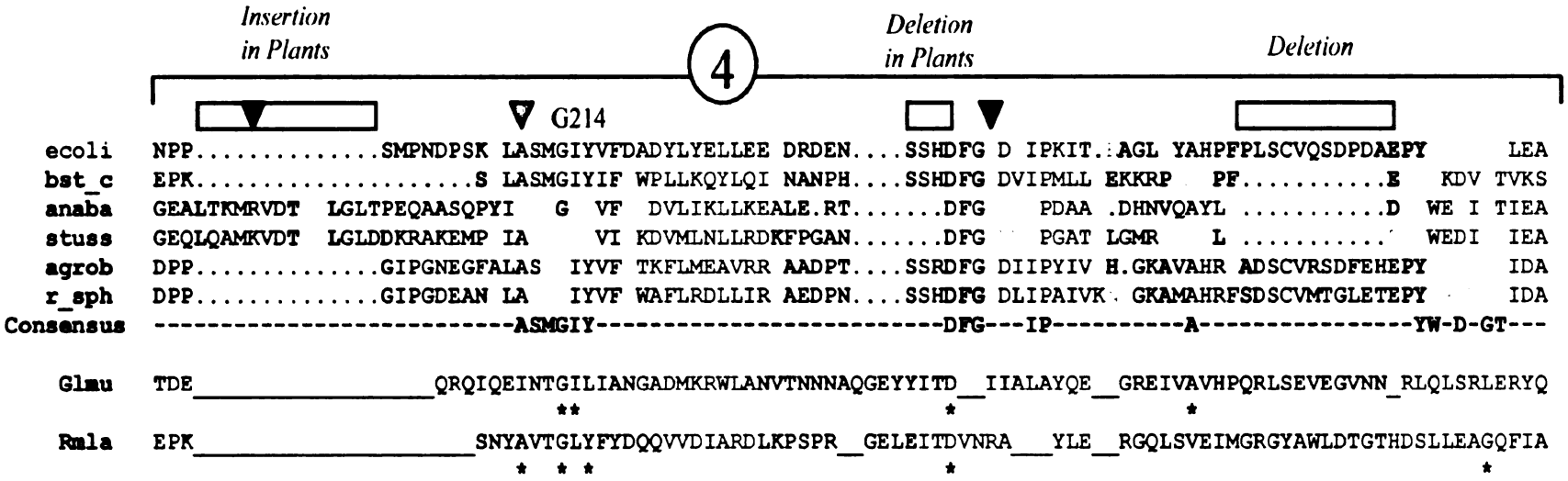

Figure 1. continued

biochemical data and the structure of the enzyme, and to possibly identify putative residues involved in catalysis.

In the current study, we present the secondary structure predictions and alignments of several ADP-Glucose PPases by the methods of PHD and a modified "Hydrophobic Cluster Anaylsis" (HCA). These predictions were compared with the solved 3-D structures of other enzymes, dTDP-glucose pyrophosphorylase (RmlA, (25)) and *N*-acetylglucosamine 1-phosphate uridyltransferase (GlmU, (26)), that catalyze the synthesis of a nucleoside diphosphate sugar. Although sequence homology of these enzymes is low in comparison to the ADP-Glc PPases, we found a definite conservation of secondary structure. Asp^{142} in *E. coli* is absolutely conserved throughout these sugar-nucleotide pyrophosphorylases and is located in a predicted loop. This same loop in RmlA and GlmU is located in the catalytic sites of these proteins. This Asp^{142} residue was mutated to an Ala, an Asn, and a Glu, and the mutant enzymes showed a substantial decrease in V_{max}, with only the Glu mutant demonstrating some variation in the K_m of the substrates and effectors. This study shows for the first time a residue from an ADP-Glc PPase that is involved in the catalysis of the enzyme.

Experimental Procedures

Materials

[^{32}P]PP_i was purchased from NEN Life Science Products. [^{14}C]Glucose-1-P was obtained from ICN Pharmaceuticals Inc. Glc-1-P, ATP, ADP-Glc, FBP, AMP, and inorganic pyrophosphatase were purchased from Sigma Chemical Co. Oligonucleotides were synthesized and purified by the Macromolecular Facility at Michigan State University. BL21(DE3) cells and Perfect™ protein markers were obtained from Novagen, Inc. The Mono Q HR 10/10 column was acquired from Amersham Pharmacia Biotech.

Construction of Plasmids and Site-Directed Mutagenesis

The pETEC plasmid was used for site-directed mutagenesis and expression of the *E. coli* wild-type and D142E mutant. It is a derivative of pET-24a (Novagen) into which the coding region of the *E. coli* ADP-Glc PPase was subcloned after PCR amplification from the plasmid pOP12 (27). The pMAB3 plasmid was utilized for expression of the D142A and D142N mutants. pMAB3 is a derivative of pMLaugh10 where the coding regions of the mutants were exchanged from the pETEC vector, after mutagenesis, using the restriction sites XbaI and SacI.

Site-directed mutagenesis was performed using the method of the Combined Chain Reaction (28). The pETEC plasmid was used as a template, and the following oligonucleotides were utilized to introduce the mutations at position 142: Asn (D142N) 5' – CTGGCGGGC**AAC**CATATCTAC – 3'; Ala (D142A) 5' – CTGGCGGGC**GCG**CATATCTAC – 3'; Glu (D142E) 5' –

CTGGCGGGC**GAA**CATATCTAC – 3'. The coding regions of the mutated plasmids were sequenced by automated dideoxy sequencing, at the Michigan State University Sequencing Facility, to confirm that no random mutations were introduced.

Expression and Purification of Wild-type and Mutant Enzymes

The wild-type and D142E plasmids were expressed in the *E. coli* bacterial strain BL21(DE3). A single colony of transformed cells was grown in Luria broth (1 L) at 37 °C up to an OD_{600} of 0.6. Induction was initiated by the addition of isopropyl-β-D-thiogalactoside (IPTG, 1 mM final concentration), with subsequent incubation at 25 °C for 4 h. The cells were then harvested and resuspended in *storage buffer* containing 20 mM potassium phosphate (pH 7.5), 5 mM dithiothreitol (DTT), and 1 mM EDTA (about 5 mL of buffer/g of cells). All subsequent protein purification steps were conducted at 0-4 °C. The resuspensions were sonicated for three 30 s intervals with cooling on ice between sonications. The sonicated suspensions were centrifuged for 15 min at 15,000 g, and the supernatants were retained. An ammonium sulfate cut (30-60%) of the supernatants was performed, with centrifugation of the cut samples for 20 min at 20,000 g. The 30-60% ammonium sulfate pellets were resuspended in 3 mL of *storage buffer* and desalted on Bio-Rad 10 DG chromatography columns equilibrated with *buffer A* (50 mM HEPES (pH 7.5), 10% sucrose, 2.5 mM DTT, and 1 mM EDTA). The desalted samples were applied individually to a Mono Q HR 10/10 column equilibrated with *buffer A*. The column was washed with 2 column volumes of *buffer A*, and the samples were eluted with a linear KCl gradient (160 mL, 0-0.5 M) in *buffer A*.

Fractions of 4 mL were collected and those containing activity were desalted in *buffer A* minus the 10% sucrose.

The D142N and D142A mutant plasmids were expressed in *E. coli* bacterial strain AC70R1-504, which is deficient in endogenous ADP-Glc PPase activity. Transformed cells (1 L) were induced as described for the plasmid pMLaugh10 (13). The mutant enzymes were purified as above.

The specific activity in the crude extracts of the wild type, D142N, D142E, and D142A enzymes were 45, 0.009, 0.5, and 0.01 units/mg, respectively. The enzymes remained stable during the purification, and the total yield was 24, 36, 37, and 21%. Since the proteins were over-expressed, to reach homogeneity (a single band stained with Coomassie Blue after 2 μg were run in a SDS-PAGE) it was necessary to purify them only 4.6-, 3.3-, 5.4-, and 4-fold, respectively.

Enzyme Assay

Assay A) Pyrophosphorolysis. Formation of [^{32}P]ATP from [^{32}P]PP_i in the direction of pyrophosphorolysis at 37 °C was determined by the method of Shen and Preiss (29). The reaction mixtures contained 80 mM HEPES (pH 7.0), 7 mM $MgCl_2$, 1.5 mM [^{32}P]PP_i (1500-2500 cpm/nmol), 2 mM ADP-Glc, 1 mM FBP, 4 mM NaF, and 0.05 mg/mL bovine serum albumin (BSA), plus enzyme in a total volume of 250 μL. The reaction mixtures for the D142E mutant were similar, except they contained 10 mM $MgCl_2$, 2 mM [^{32}P]PP_i, and 3 mM FBP to compensate for increased K_m values.

Assay B) Synthesis. Formation of [^{14}C]ADP-glucose from [^{14}C]Glc-1-P in the synthesis direction at 37 °C was determined by the method of Preiss *et al.* (7). The

reaction mixtures consisted of 100 mM HEPES (pH 7.6), 6 mM $MgCl_2$, 0.5 mM [^{14}C]Glc-1-P (~1000 cpm/nmol), 1 mM ATP, 2 mM FBP, 0.0015 U/μL pyrophosphatase, and 0.2 mg/mL BSA, plus enzyme in a total volume of 200 μL. The reaction mixtures for the D142E mutant were similar, except they contained 12 mM $MgCl_2$, 3 mM [^{14}C]Glc-1-P (~300 cpm/nmol), 6 mM ATP, and 3 mM FBP. When measuring the kinetic value of the inhibitor, AMP, for the wild-type and D142A and D142N mutants, 1.5 mM FBP was present in the assay mixture. The FBP concentration in the same inhibitor assay mixture was increased to 3 mM for the D142E mutant.

One unit of enzyme activity in the above assays is equal to 1 μmol of product, either [^{32}P]ATP or [^{14}C]ADP-glucose, formed per minute at 37 °C.

Kinetic Characterization

The kinetic data were plotted as initial velocity (nmol/min) versus substrate or effector concentration (mM). The kinetic constants were acquired by fitting the data with a non-linear least square formula and the Hill equation using the program Origin™ 5.0. The Hill coefficient, n_H, and the kinetic constants, $S_{0.5}$, $A_{0.5}$, and $I_{0.5}$, which correspond to the concentration of substrate, activator or inhibitor giving 50% of the maximal velocity, activation, or inhibition, respectively, were calculated from the Hill plots.

Protein Assay

Enzyme concentration during protein purification was measured by using bicinchoninic acid reagent (30) from Pierce Chemical Company, with BSA as the

standard. Protein concentration of the purified enzymes was determined by UV absorbance at 280 nm using an extinction coefficient of 1.0.

Protein Electrophoresis and Immunoblotting

Protein purification was monitored by SDS-PAGE as described by Laemmli (31), utilizing 4-15% Tris-HCl pre-cast gradient polyacrylamide gels from Bio-Rad. Perfect™ protein markers were used for molecular weight standards. Following electrophoresis, protein bands were either visualized by staining with Coomassie Brilliant Blue R-250 or electroblotted onto a Protran™ (Schleicher & Schuell) nitrocellulose membrane. The nitrocellulose membrane was subsequently treated with affinity-purified anti-*E. coli* B strain AC70R1 ADP-Glc PPase IgG (9). The resulting antigen-antibody complex was visualized by treatment with alkaline phosphatase-linked goat anti-rabbit IgG, then staining with BM purple AP-substrate precipitating reagent from Boehringer Mannheim Corp.

Stability of the Enzymes to Heat

An aliquot, 15 μg, of the purified enzymes was diluted (1:2) in a 0.5 mL microcentrifuge tube containing the following enyzme dilution buffer: 50 mM HEPES (pH 8.0), 10% sucrose, 5 mM $MgCl_2$, 0.1 mM EDTA, and 2 mg/mL BSA (total volume: 30 μl). The heat treatment was performed at 55 °C for 5 min with subsequent cooling on ice. Aliquots were then removed to measure the activity using assay B. A control without heat treatment was analyzed in parallel for comparison (100% activity).

Structure Prediction Analysis

The amino acid sequence of the ADP-Glc PPases was analyzed by a profile neural network program (PHD program (32)) to predict the secondary structure and the probability for the residues to be exposed. Sequences were aligned manually based on the primary and predicted secondary structure. A modified two-step method of "Hydrophobic Cluster Analysis" was used to enhance the alignment (33). The original method plotted clusters of amino acids as an α-helix, and the hydrophobic ones were highlighted and encircled to signal the presence of a hydrophobic cluster. In our method, we encircled clusters of residues predicted as "buried" by the PHD program. To expedite this process, we developed a program in Pascal language (unpublished results). This modified method of HCA proved to be more accurate in finding similar clusters in these homologous proteins.

Results

Prediction of the structure and alignment of ADP-Glc PPases. The catalytic reactions of RmlA and GlmU are similar to ADP-Glc PPase. The 3-D structures of the former enzymes have been solved (25,26), but the homology to the ADP-Glc PPases is low: 15% identity between the *E. coli* ADP-Glc PPase and the pyrophosphorylase domain of GlmU. To verify that ADP-Glc PPases share a common structure and to improve the protein sequence alignment, the secondary structures of several ADP-Glc PPases were predicted. For this prediction, ADP-Glc PPases were selected from different sources, i.e., *E. coli*, *Anabaena*, *Chlamydomonas reinhardtii*, potato tuber "small" subunit, and different "large" subunits from maize embryo, maize *shrunken 2*, and *Arabidopsis thaliana*. Each protein represented various classes according to the homology of the subunits and the types of regulation and tissue. The first step was to confirm that the ADP-Glc PPases from different sources share a common structure in spite of their diversity. A modified method of "Hydrophobic Cluster Analysis" (33) was applied to these enzymes. HCA showed that the ADP-Glc PPases are extremely similar in the distribution and pattern of the hydrophobic clusters even between bacterial and plant enzymes (data not shown). This strongly suggests that the ADP-Glc PPases share a common folding pattern, despite differences in quaternary structure ($\alpha_2\beta_2$ in plants and α_4 in bacteria) and in specificity for the activator.

If the ADP-Glc PPases from different sources have a similar 3-D structure, their secondary structure predictions should also be similar. All the sequences mentioned above, including those from *Agrobacterium tumefaciens*, *Bacillus stearothermophilus*, and *Rhodobacter sphaeroides*, were analyzed using the PHD program to predict the

secondary structure (32). Processing several sequences helped to establish a structure for aligned regions where the confidence of the prediction for α-helices or β-sheets was low for one of the enzymes but high for the rest (Figure 1). Also of importance was the prediction of loops, which are assigned by the PHD program when the likelihood of either α-helices or β-sheets is low. To enhance the prediction of the loops, we used the following biochemical and genetic data:

i) Exposed loops are more sensitive to proteolytic cleavage. Proteolytic studies on ADP-Glc PPase confirmed that proteases cut in sites predicted as loops or very close to them (Figure 1). The exceptions were two cuts in an α-helix predicted near the C-terminal of the *Anabaena* enzyme (data not shown) and in a β-sheet (Met^{181}-Ala^{182}, Figure 1). Since the α-helix is an insertion (20 amino acids) that is absent in the enzyme from *E. coli* and is not predicted as "buried" by the PHD program, it is most likely that this helix is not part of the core but rather a part of a loop in a domain of 8 β-sheets. The β-sheet, which is the second one in region 3, is probably in an exposed region. To support this hypothesis, in GlmU the equivalents of the second and third β-sheets of region 3 are not part of the core of the protein (26).

ii) During evolution, loops in homologous proteins are prone to insertions and deletions without altering the overall structure of the proteins. In the prediction, all of the insertions and deletions observed among sequences from different sources fell in the predicted loops (Figure 1).

iii) The conserved amino acids known to have specific roles in the binding of substrates (*E. coli* Tyr^{114}, Lys^{195}) and of activators (*E. coli* Lys^{39}, *Anabaena* Lys^{382}, Lys^{419}) are located in the predicted loops. Residues P^{295} and G^{336}, which are located in a

region that is apparently important for the regulation of the *E. coli* enzyme (34,35), are also in loops.

iv) It has been observed in catalytic α/β domains that functional loops are located at the C-terminus of the β-sheets. The loops after these C-termini in regions 1, 2, and 3 contain the most amino acids that are conserved among the ADP-Glc PPases. Moreover, amino acid residues located at loops that are at the N-terminus of β-sheets in regions 2 and 3 are not conserved at all. The only exception is in region 1. However, there is evidence from chemical modification and site directed mutagenesis that this loop interacts with the activator FBP in the ADP-Glc PPase from *E. coli* (16,17).

Taking the above information into consideration, the protein sequences of the ADP-Glc PPases were aligned manually with the sequences of RmlA and of the pyrophosphorylase domain of GlmU. The secondary structure of the predicted model is extremely similar to the secondary structures of these structurally solved proteins.

Expression and purification of the wild-type and mutant enzymes. The expression of the D142 mutant enzymes was similar to the wild-type enzyme as determined by Western blot (data not shown). Thus, either the BL21(DE3) or the AC70R1-504 expression systems were efficient at over-expressing the recombinant ADP-Glc PPases. The drawback to using the BL21(DE3) expression system is the presence of an endogenous ADP-Glc PPase activity, which might interfere with an accurate determination of the kinetic parameters of the mutants D142N and D142A because of the significant decrease in their catalytic activity.

The Mono-Q fractions of the wild-type and mutant enzymes were analyzed by SDS-PAGE and showed a single band for each sample corresponding to a molecular

weight of about 50 kDa (data not shown). The homogeneous enzymes were then used for kinetic analyses.

Kinetic characterization of the wild-type and mutant enzymes. The mutant enzymes were assayed both in the synthesis and the pyrophosphorolysis directions, as described in the Experimental Procedures (assays A and B), to compare the kinetic parameters of the mutant enzymes with the wild-type. The values of the kinetic parameters reported here for the wild-type are in good agreement with those previously reported (e.g. (18)).

In the direction of synthesis, the apparent substrate affinities ($S_{0.5}$) for the D142N and D142A mutants were not significantly different from the values measured for the wild-type (Table I). In contrast, the substrate values for the D142E mutant were altered in comparison to the wild-type, showing a 47-fold increase for Glc-1-P $S_{0.5}$, an 11.5-fold increase for ATP $S_{0.5}$, and a 2-fold increase for Mg^{2+} $S_{0.5}$ (Table I). The D142E mutant also had an increased Hill coefficient (n_H) for Glc-1-P (2-fold), showing increased cooperativity for this substrate.

The mutation of D142 to Asn and Ala did not seem to affect the ability of the mutant enzymes to bind the activator, FBP. The FBP $A_{0.5}$ values for the D142N and D142A mutants decreased 3- and 2-fold, respectively (Table I). Both mutants were activated by 5- and 7-fold, respectively, whereas the wild-type was activated by 9-fold (data not shown). On the other hand, the $A_{0.5}$ for FBP increased 17-fold for the D142E mutant in comparison to the wild-type (Table I). The activation by FBP was >100-fold since the activity in the absence of activator was barely detectable (data not shown).

Table I. Kinetic parameters of *E. coli* wild-type and mutant ADP-glucose pyrophosphorylases in the synthesis direction[a]

	Glc-1-P		ATP		Mg^{2+}		FBP		AMP	
	$S_{0.5}$ (mM)	n_H	$S_{0.5}$ (mM)	n_H	$S_{0.5}$ (mM)	n_H	$A_{0.5}$ (mM)	n_H	$I_{0.5}$ (mM)	n_H
wt	0.018 ± 0.004	0.9	0.26 ± 0.03	1.8	2.17 ± 0.08	4.8	0.03 ± 0.01	1.9	0.04 ± 0.01	1.7
D142N	0.024 ± 0.008	1.2	0.14 ± 0.01	1.7	1.76 ± 0.05	3.6	0.009 ± 0.001	1.4	1.0 ± 0.1	1.2
D142E	0.84 ± 0.09	1.9	3.0 ± 0.3	2.1	5.01 ± 0.08	3.2	0.50 ± 0.01	2.2	0.06 ± 0.01	1.3
D142A	0.015 ± 0.004	1.4	0.15 ± 0.01	1.7	1.76 ± 0.05	3.9	0.016 ± 0.001	1.8	0.13 ± 0.02	1.2

[a] Reactions were performed at 37 °C using assay B as described under "Experimental Procedures." The data represent the mean of two independent experiments with the difference expressed as a ± deviation.

The inhibition by AMP showed no significant changes for the D142E mutant and only a small increase (3 fold) in the AMP $I_{0.5}$ value for the D142A mutant in comparison to the wild-type. However, the $I_{0.5}$ value for the D142N mutant increased by 25-fold (Table I).

In the direction of pyrophosphorolysis, the D142N and D142A mutants showed only minor variations in the values obtained for the apparent substrate affinities in comparison to the wild-type (Table II). As observed in the synthesis direction, the apparent substrate affinities for the D142E mutant were increased from those measured for the wild-type (Table II). The ADP-Glc $S_{0.5}$, the PP_i $S_{0.5}$, and the Mg^{2+} $S_{0.5}$ values were increased 4-, 11-, and 2-fold, respectively. The FBP $A_{0.5}$ values for the D142N, D142E, and D142A mutants were increased 6-, 13-, and 5-fold over the wild-type (Table II).

The most dramatic variations of the mutant enzymes from the wild-type were observed in the determination of the specific activities of the mutants (Table III). The D142E mutant showed a decrease of around 2 orders of magnitude when compared to the wild-type in either the direction of synthesis or pyrophosphorolysis. This decrease in specific activity became even larger for the D142N and D142A mutants, approaching 4 orders of magnitude in either direction, synthesis or pyrophosphorolysis.

Thermal stability of the Asp^{142} mutants. After heat treatment at 55°C for 5 min, the remaining activity of the wild type enzyme was 80%; whereas, the mutants D142A, D142E, and D142N retained 98, 96, and 52% of the initial activity, respectively. Only the Asn mutant showed a decrease in initial activity, indicating that Asp^{142} is not required for the stability of the enzyme.

Table II. Kinetic parameters of *E. coli* wild-type and mutant ADP-glucose pyrophosphorylases in the pyrophosphorolysis direction[a]

	ADP-Glc		PP_i		Mg^{2+}		FBP	
	$S_{0.5}$ (mM)	n_H	$S_{0.5}$ (mM)	n_H	$S_{0.5}$ (mM)	n_H	$A_{0.5}$ (mM)	n_H
wt	0.11 ± 0.01	1.8	0.11 ± 0.03	0.8	1.61 ± 0.05	2.5	0.015 ± 0.001	1.8
D142N	0.18 ± 0.02	1.8	0.16 ± 0.08	1.6	1.7 ± 0.1	2.7	0.088 ± 0.002	1.8
D142E	0.46 ± 0.02	2.3	1.2 ± 0.2	1.3	3.9 ± 0.2	2.0	0.20 ± 0.04	2.2
D142A	0.054 ± 0.002	1.9	0.05 ± 0.01	1.1	1.8 ± 0.1	2.6	0.081 ± 0.004	1.9

[a] Reactions were performed at 37 °C using assay A as described under "Experimental Procedures." The data represent the mean of two independent experiments with the difference expressed as a ± deviation.

Table III. Comparison of specific activities of the *E. coli* wild-type and mutant ADP-glucose pyrophosphorylases[a]

		V_{max} (U/mg)	Fold Decrease
Synthesis			
	E. coli wt	209	-
	D142N	0.029	7200
	D142A	0.038	5500
	D142E	2.71	77
Pyrophosphorolysis			
	E. coli wt	210	-
	D142N	0.020	10500
	D142A	0.031	6800
	D142E	2.14	100

[a] Reactions were performed at 37 °C as stated under "Experimental Procedures." The assay conditions for the D142E mutant were altered to compensate for the increased K_m values. The data represent the mean of two independent experiments, and the differences were less than 5% error. Values were in good agreement with the V_{max} obtained in the saturated region of the substrate curves (Tables I and II).

Discussion

The 3-D structure of an enzyme is a valuable tool for analyzing the residues located in the ligand binding sites and for studying the structure-function relationships and the evolution of homologous domains in enzymes. Unfortunately, no structure of any ADP-Glc PPase has been solved yet. Two enzymes that share a similar catalytic reaction with the ADP-Glc PPase have been crystallized, and their structures have been solved (RmlA and GlmU). However, the homology with ADP-Glc PPase is very low and computer modeling is not possible. To study the structure-function relationship of a putative catalytic domain of the ADP-Glc PPase from *E. coli*, we made a prediction of the secondary structure, and the helices, loops and sheets were matched with the structures of RmlA and GmlU. The prediction was extremely similar to these proteins, enhancing the significance of highly conserved residues that were isolated. These residues were found to be in key regions of particular motifs (Figure 1). Interestingly, structures usually observed in proteins that bind nucleotides were found to be compatible with the prediction. Region 1 (Figure 1) has a glycine rich loop after a β-sheet that is similar to the "P loop" in protein kinases or nucleotide binding sites (36), and region 2 has three predicted β-sheets and helices that are compatible with the Rossman fold (37). Thus, regions 1 and 2 comprise a putative domain or subdomain that binds ATP. Moreover, Tyr^{114}, which was shown to be reactive to the azido analog of ATP (38,39), is in this region. These predictions are in excellent agreement with the 3-D structures of the RmlA and GlmU enzymes.

The secondary structure of the predicted model is extremely similar to the secondary structure of RmlA and of the pyrophosphorylase domain of the bifunctional

enzyme from GlmU. Regions 2, 3, and 4 are virtually identical. In region 4, the only difference is that two β-sheets were predicted rather than one because of the presence of Gly^{214} (breaker, Figure 1). In GlmU, this is only one β-sheet, which is bent because of a glycine and is part of the substrate site where the sugar-phosphate rests. Possibly, this motif is typical of the pyrophosphorylase family. The only area that the predicted secondary structures of other pyrophosphorylases, such as GDP-Man PPases, CDP-Glc PPases, and UDP-Glc PPases, did not match was the last ten residues of region 1 and the first ten residues of region 2 (data not shown).

There are other loops in the structures of GlmU and RmlA that face their respective substrates. In the prediction of the structure of the ADP-Glc PPases we found that there are highly conserved residues in these homologous loops (Figure 1). Some of them have already been assigned a function. For instance K^{195}, the Glc-1-P binding site in ADP-Glc PPases, is present in the third loop of region 3 and interacts with the sugar-phosphate in both RmlA and GlmU. The homologous lysine is present in RmlA and in GlmU but shifted one position in the latter. The fourth loop in region 2 (Figure 1) has residues that are conserved in the ADP-Glc PPases and that interact with the dTTP or UTP in RmlA and GlmU, respectively. It contains Tyr^{114}, which has been proposed to be close to the ATP binding site. Also, the last residue of this loop is Gly^{116} which is part of the motif "GTAD" that is highly conserved in ADP-Glc PPases. Most probably the function of this loop is to confer the specificity for the nucleotide since these residues interact with the base. Asp^{142} in ADP-Glc PPase from *E. coli* is another one of these highly conserved residues that is located in a loop predicted to be near the substrates by comparison with RmlA and GlmU. In this study the function of this residue was

analyzed by site-directed mutagenesis. Replacement of Asp^{142} resulted in a significant decrease in catalysis in either direction of product formation. This effect on catalysis was reduced by conserving the negative charge (Glu, Table III), indicating that the charge of this residue plays an important role in the catalytic reaction. The possibility that the activity measured for this D142E mutant was contaminated with the endogenous ADP-Glc PPase from the BL21(DE3) expression system was ruled out by comparing with a control of the cell with the pET-24a vector alone. In the crude extract of the D142E mutant, the endogenous contamination accounted for <0.1% of the total specific activity (data not shown). Moreover, the substrate and ligand binding curves for the D142E mutant were unique in comparison to the wild-type, i.e. they were not a composite of the two enzymes.

This is the first time that a residue involved in the catalysis of an ADP-Glc PPase enzyme has been characterized. Although the activity of the D142N and D142A mutants was reduced by 4 orders of magnitude, we were still able to obtain data on the other kinetic parameters of these mutant enzymes. Measuring the effect of mutations on catalytic residues can be limiting when the activity of the mutant enzyme(s) falls below the sensitivity of the assay. Blankenfeldt *et al.* (2000) mutated the corresponding Asp residue in RmlA based on their determination of the 3-D structure of the enzyme and their results show a decrease in catalytic activity of at least 3 orders of magnitude for the mutated enzymes. However, they were not able to measure any other kinetic parameters, providing them with only partial information about this residue in RmlA.

Even though mutation of Asp^{142} most significantly affected the catalysis of ADP-Glc PPase from *E. coli*, to a lesser extent the mutation affected the regulation of the

D142E and D142N mutants (Table I). As discussed above, the $A_{0.5}$ for FBP of D142E increased 17-fold and the $I_{0.5}$ for AMP of D142N increased 25-fold over wild-type. These changes can be attributed to a suboptimal interaction between the regulatory and the catalytic sites through a disruption of the local environment surrounding Asp^{142}. The mutation of Asp^{142} to Glu does not alter the charge. However, there is an extra methylene in Glu that probably interferes with the normal interaction of this negatively charged residue with those residues that might be important for regulation. In fact, the activator of ADP-Glc PPase from *E. coli* interacts with Lys^{39}, which was predicted to be in a loop by the PHD program (Figure 1). This loop is predicted to be near Asp^{142} in the tertiary conformation of the enzyme from the alignment with the proteins RmlA and GlmU. The location of the inhibitor binding site is not known for the *E. coli* ADP-Glc PPase, however it could be in the same vicinity of these residues in the native enzyme. Since the regulation of the ADP-Glc PPase enzyme from *E. coli* is allosteric, any changes in the affinity for one effector can alter the affinity for the other, which suggests the binding sites are close in proximity. This allosteric relationship has been studied in *E. coli* (40) and in other ADP-Glc PPase enzymes as well (e.g. (4,41,42)), demonstrating the sensitivity of each effector to changes in the concentration of the other.

The exact role Asp^{142} plays in the catalytic mechanism of ADP-Glc PPase from *E. coli* is unknown. A detailed chemical mechanism of the residues involved in the catalysis of ADP-Glc PPase has not been elucidated; however, the kinetic reaction has been studied. A kinetic mechanism for ADP-Glc PPase was first analyzed in *Rhodospirillum rubrum*, from which an ordered bi bi mechanism is favored over a Theorell-Chance mechanism (43). The kinetic mechanism of ADP-Glc PPase from

E. coli B was found to be similar to *R. rubrum*, reinforcing a sequential binding of ATP followed by glucose-1-P (44). Study of other sugar-nucleotide PPase mechanisms has also indicated a sequential binding order of substrates (e.g. (45-47)). The solution of the 3-D structures of the RmlA and GlmU enzymes, which share a similar reaction to ADP-Glc PPases of forming a sugar-nucleotide product, provides some insight to the results of this study. Based on their results from the crystallized RmlA, Blankenfeldt *et al.* (2000) proposed a chemical mechanism that proceeds by an S_N2 reaction, in which the Asp^{142} residue is directly involved (Asp^{110} in RmlA). They suggest that the Asp activates the α-phosphate of the nucleotide for nucleophilic attack by the sugar-phosphate. In contrast, the pyrophosphorylase domain from the solved GlmU structure shows the homologous Asp to be located in a position that is closer to the ribose moiety of the nucleotide, and the authors suggest that it is involved in the binding of the UTP substrate (26). This contradicts the findings for RmlA and does not support our results for the site-directed mutagenesis of Asp^{142}. Furthermore, our results show this residue to be important in both directions of the catalytic reaction, strongly suggesting the involvement of Asp^{142} in the catalysis of the enzyme.

The 3-D structure of RmlA supports our results showing for the first time a residue involved in the catalysis of an ADP-Glc PPase enzyme. The secondary structure of RmlA, as well as of the GlmU enzyme, is very similar to the predictions for the ADP-Glc PPases. In particular, the alignment of these enzymes shows a pattern of conserved residues among the different pyrophosphorylases (Figure 1). This suggests that there is a sharing of a common pyrophosphorylase domain among these enzymes (Figure 2). Within this domain, there are also residues particular to each type of sugar-

phosphate and nucleotide substrate that are not conserved in the other types of pyrophosphorylases (e.g., the Tyr^{114} residue from *E. coli* which interacts with the adenine-ring of the ATP substrate for ADP-Glc PPase (14)). Interestingly, most of the residues involved in the regulation of the ADP-Glc PPases are located outside this conserved domain. As was mentioned earlier, this area has diverged even among the class of ADP-Glc PPases. It might be suggested that the variation in the sizes of the N- and C-terminal regions among these different classes of enzyme is related to the specifics of regulation, if any, for individual classes. Further studies of the ADP-Glc PPases and the other sugar-nucleotide pyrophosphorylases are needed to fully comprehend their relationships with one another.

Figure 2. Comparison of the pyrophosphorylase domain of various classes of enzymes that catalyze the synthesis of a sugar-nucleotide. The classes are represented by sequences obtained from GenBank that were used in the predictions of the secondary structures by PHD. The gray region is defined by the consensus sequence markers beginning with GG_G(S/T)R and ending with EKP. Represented in light gray is a region that might complete the substrate-binding pocket of the pyrophosphorylase domain, extending through the first β-sheet of region 4 and including Gly^{214}. The numbers of amino acids in the N- and C-terminal regions surrounding the pyrophosphorylase domain are averaged for each class of enzyme (figure not to scale).

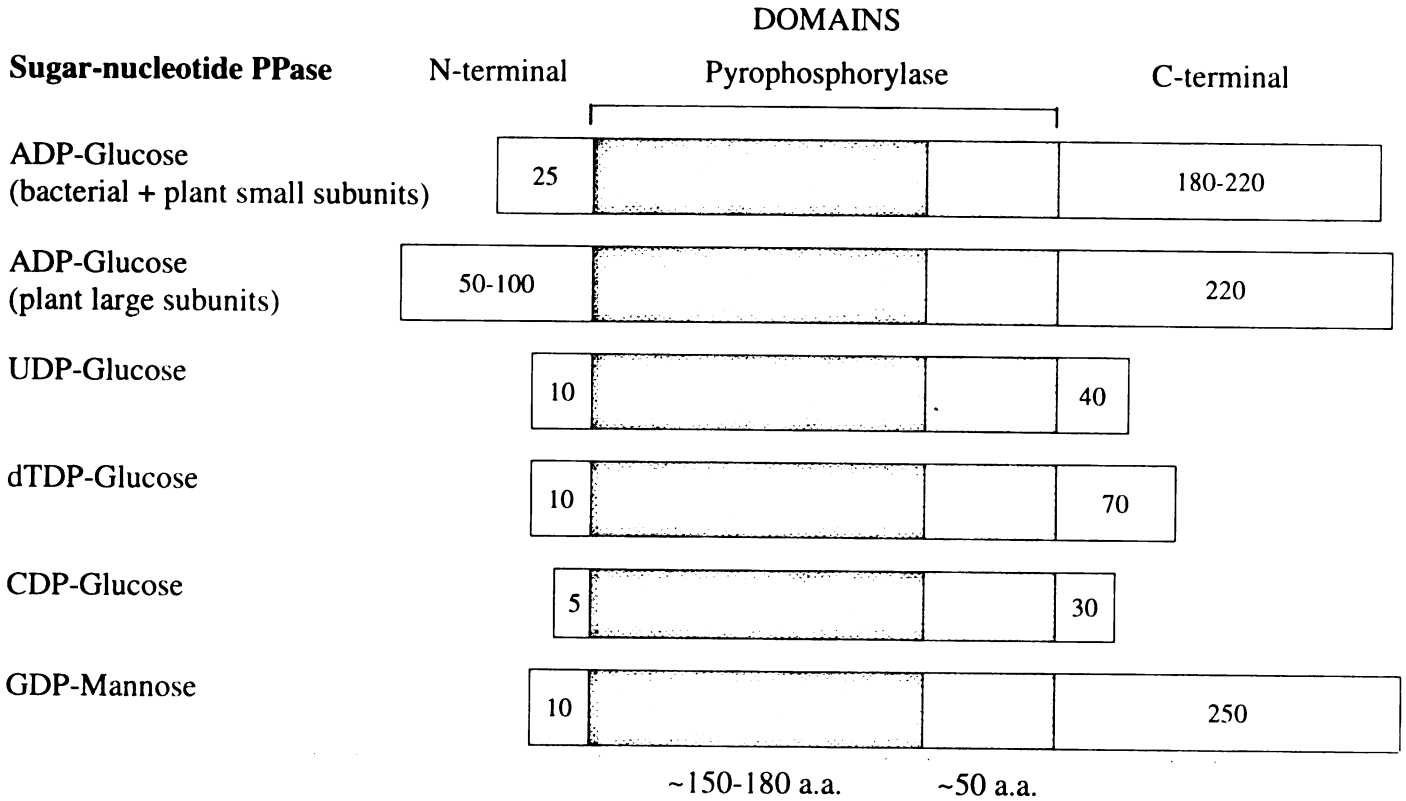
DOMAINS
Sugar-nucleotide PPase
N-terminal
Pyrophosphorylase
C-terminal
ADP-Glucose
(bacterial + plant small subunits)
25
180-220
ADP-Glucose
(plant large subunits)
50-100
220
UDP-Glucose
10
40
dTDP-Glucose
10
70
CDP-Glucose
5
30
GDP-Mannose
10
250
~150-180 a.a.
~50 a.a.

Figure 2.

References

1. Espada, J. (1962) *J. Biol. Chem.* **237,** 3577-3581
2. Preiss, J. (1984) *Annu. Rev. Microbiol.* **38,** 419-458
3. Preiss, J., and Sivak, M. N. (1998) in *Comprehensive Natural Products Chemistry* (Pinto, B. M., ed) Vol. 3, pp. 441-495, Pergamon Press, Oxford
4. Ghosh, H. P., and Preiss, J. (1966) *J. Biol. Chem.* **241,** 4491-4504
5. Sivak, M. N., and Preiss, J. (1998) in *Adv. Food Nutr. Res.* (Taylor, S. L., ed) Vol. 41, pp. 1-199, Academic Press, San Diego
6. Preiss, J. (1973) in *The Enzymes* (Boyer, P. D., ed) Vol. 8, pp. 73-119, Academic Press, New York
7. Preiss, J., Shen, L., Greenberg, E., and Gentner, N. (1966) *Biochemistry* **5,** 1833-1845
8. Ozaki, H., and Preiss, J. (1972) *Methods Enzymol.* **28,** 406-413
9. Haugen, T. H., Ishaque, A., and Preiss, J. (1976) *J. Biol. Chem.* **251,** 7880-7885
10. Morell, M. K., Bloom, M., Knowles, V., and Preiss, J. (1987) *Plant Physiol.* **85,** 182-187
11. Preiss, J. (1991) in *Oxford Surveys of Plant Molecular and Cell Biology* (Mifflin, B., ed) Vol. 7, pp. 59-114, Oxford University Press, Oxford
12. Krishnan, H. B., Reeves, C. D., and Okita, T. W. (1986) *Plant Physiol.* **81,** 642-645
13. Ballicora, M. A., Laughlin, M. J., Fu, Y., Okita, T. W., Barry, G. F., and Preiss, J. (1995) *Plant Physiol.* **109,** 245-251.

14. Kumar, A., Tanaka, T., Lee, Y. M., and Preiss, J. (1988) *J. Biol. Chem.* **263,** 14634-14639.

15. Parsons, T. F., and Preiss, J. (1978) *J. Biol. Chem.* **253,** 6197-6202.

16. Parsons, T. F., and Preiss, J. (1978) *J. Biol. Chem.* **253,** 7638-7645.

17. Gardiol, A., and Preiss, J. (1990) *Arch. Biochem. Biophys.* **280,** 175-180.

18. Hill, M. A., Kaufmann, K., Otero, J., and Preiss, J. (1991) *J. Biol. Chem.* **266,** 12455-12460.

19. Fu, Y., Ballicora, M. A., and Preiss, J. (1998) *Plant Physiol.* **117,** 989-996.

20. Morell, M., Bloom, M., and Preiss, J. (1988) *J. Biol. Chem.* **263,** 633-637.

21. Ball, K., and Preiss, J. (1994) *J. Biol. Chem.* **269,** 24706-24711.

22. Charng, Y. Y., Iglesias, A. A., and Preiss, J. (1994) *J. Biol. Chem.* **269,** 24107-24113

23. Ballicora, M. A., Fu, Y., Nesbitt, N. M., and Preiss, J. (1998) *Plant Physiol.* **118,** 265-274.

24. Smith-White, B. J., and Preiss, J. (1992) *J. Mol. Evol.* **34,** 449-464

25. Blankenfeldt, W., Asuncion, M., Lam, J. S., and Naismith, J. H. (2000) *EMBO J.* **19,** 6652-6663.

26. Brown, K., Pompeo, F., Dixon, S., Mengin-Lecreulx, D., Cambillau, C., and Bourne, Y. (1999) *EMBO J.* **18,** 4096-4107.

27. Okita, T. W., Rodriguez, R. L., and Preiss, J. (1981) *J. Biol. Chem.* **256,** 6944-6952

28. Bi, W., and Stambrook, P. J. (1998) *Anal. Biochem.* **256,** 137-140.

29. Shen, L., and Preiss, J. (1964) *Biochem. Biophys. Res. Commun.* **17,** 424-429

30. Smith, P. K., Krohn, R. I., Hermanson, G. T., Mallia, A. K., Gartner, F. H., Provenzano, M. D., Fujimoto, E. K., Goeke, N. M., Olson, B. J., and Klenk, D. C. (1985) *Anal. Biochem.* **150,** 76-85

31. Laemmli, U. K. (1970) *Nature* **227,** 680-685

32. Rost, B., and Sander, C. (1993) *Proc. Natl. Acad. Sci. U. S. A.* **90,** 7558-7562.

33. Lemesle-Varloot, L., Henrissat, B., Gaboriaud, C., Bissery, V., Morgat, A., and Mornon, J. P. (1990) *Biochimie* **72,** 555-574

34. Ghosh, P., Meyer, C., Remy, E., Peterson, D., and Preiss, J. (1992) *Arch. Biochem. Biophys.* **296,** 122-128.

35. Meyer, C. R., Ghosh, P., Remy, E., and Preiss, J. (1992) *J. Bacteriol.* **174,** 4509-4512.

36. Saraste, M., Sibbald, P. R., and Wittinghofer, W. (1990) *Trends Biochem. Sci.* **15,** 430-434

37. Rossman, M. G., Moras, D., and Olsen, K. W. (1974) *Nature* **250,** 194-199

38. Lee, Y. M., and Preiss, J. (1986) *J. Biol. Chem.* **261,** 1058-1064.

39. Lee, Y. M., Mukherjee, S., and Preiss, J. (1986) *Arch. Biochem. Biophys.* **244,** 585-595.

40. Gentner, N., and Preiss, J. (1967) *Biochem. Biophys. Res. Commun.* **27,** 417-423.

41. Sanwal, G. G., and Preiss, J. (1967) *Arch. Biochem. Biophys.* **119,** 454-469.

42. Sowokinos, J. R., and Preiss, J. (1982) *Plant Physiol.* **69,** 1459-1466

43. Paule, M. R., and Preiss, J. (1971) *J. Biol. Chem.* **246,** 4602-4609

44. Haugen, T. H., and Preiss, J. (1979) *J. Biol. Chem.* **254,** 127-136.

45. Neufeld, E. F., Ginsburg, V., Putman, E. W., Fanshier, D., and Hassid, W. Z. (1957) *Arch. Biochem. Biophys.* **69,** 602-616

46. Tsuboi, K. K., Fukunaga, K., and Petricciani, J. C. (1969) *J. Biol. Chem.* **244,** 1008-1015.

47. Melo, A., and Glaser, L. (1965) *J. Biol. Chem.* **240,** 398-405

48. Wu, M. X., and Preiss, J. (1998) *Arch. Biochem. Biophys.* **358,** 182-188.

CHAPTER 4

RESEARCH PERSPECTIVES

The work presented in Chapters 2 and 3 has focused primarily on site-directed mutagenesis as a means of elucidating information about residues involved in the function of ADP-glucose pyrophosphorylase (ADP-Glc PPase). Of course there are many other techniques, e.g. chemical modification and crystallography, that can be used in the place of or in combination with site-directed mutagenesis to provide important information about the structure/function relationships of proteins.

The study of the inhibitor specific residue Arg^{294} in ADP-Glc PPase from *Anabaena* gave interesting results on many levels. First, it demonstrated that for inhibition by orthophosphate (P_i) to occur, the enzyme specifically required an arginine. This was of basic interest whether it was the size or charge or both involved in the interaction, since only an alanine substitution was studied at first. A more intriguing finding about the mutations at Arg^{294}, is the change in inhibitor specificity for the R294A and R294Q mutants to NADPH instead of P_i. For the wild-type enzyme, this inhibition may have no physiological relevance because of the high $I_{0.5}$ for NADPH, around 5 mM. It is very interesting though that a single mutation can affect the conformation of the inhibitor site, allowing the much larger NADPH to fit better than the P_i. Obviously it would be very helpful to have a 3-D structure of the enzyme to help interpret these results since we have no idea what the inhibitor site looks like. However, there was an interesting result from the analysis of NADPH inhibition on the wild-type enzyme in the absence of 3-phosphoglycerate (Chapter 2, Figure 2A) that might offer some insight into the structure of the enzyme. At low concentrations of NADPH ($\leq$1 mM), the wild-type enzyme was actually activated by NADPH, and then it started to inhibit the enzyme. This triphosphopyridine nucleotide compound shares structural features with other

compounds that are either substrates for, i.e. ATP or ADP-glucose, or effectors of, e.g. fructose-1,6-bisphosphate, ADP-Glc PPases. It is a possibility that the NADPH is interacting at other sites, besides the inhibitor site, to give some kind of mixed competition. In fact, if the substrate binding and inhibitor binding sites are close enough in 3-D space, maybe the NADPH molecule could be occupying both, i.e. the ADP portion in the substrate site and the 2'-ribosyl phosphate in the inhibitor site. Future study of the wild-type and the R294A and R294Q should be done to look at the specifics of the interaction of NADPH with these enzymes.

The study of aspartic acid residue 142 showed that this residue is involved in the catalysis of the ADP-Glc PPase from *E. coli*. Some activity was retained with the conservative substitution to glutamic acid, indicating that the negative charge plays a role in the catalysis. Mutation of this residue would not have been pursued without some initial work that concentrated on making a structural model of this enzyme. Assembling models of the primary and secondary structures of the different ADP-Glc PPases has aided many researchers in our laboratory in the study of these enzymes. The recent publication of the solved crystal structures of two enzymes, RmlA (1) and GlmU (2), that share a common reaction of sugar-nucleotide synthesis with our ADP-Glc synthesizing enzyme, has helped add some support to our structural predictions (Chapter 3, Figure 1). The structural data from the RmlA and GlmU enzymes fit quite well to our model that was predicted using the PHD program. Aligning these sequences by the structures and structural predictions, facilitated the discovery of some residues that are conserved among the different enzymes even though the overall homology is very low. One of those residues is Asp^{142}, which was demonstrated to be involved in catalysis. Some of

the other conserved residues found by this alignment should be analyzed. Of particular interest would be the highly conserved N-terminal motif GG_G(S/T)R, which is similar to the phosphate binding portion of nucleotide-binding proteins. Obviously, one must be careful when drawing any conclusions from the comparison of a predicted structure and the solved structure of a similar but not exactly the same enzyme. However, when a solved structure of the enzyme of you are studying does not yet exist, other techniques to study the structure should be explored and might help in understanding the structure/function relationships of the enzyme.

By no means is the study of the ADP-Glc PPase enzyme complete. The solved 3-D structure of at least one of the ADP-Glc PPases will help in the interpretation of the existing biochemical data. Recent progress has been made in this area (3); however, there are other questions remaining about the enzyme that the 3-D structure alone may not be able to answer. One example is does the large subunit have any catalytic activity? An interesting experiment that should be done is to mutate the residues in the small and large subunits of the enzyme from plants that are homologous to Asp^{142} in *E. coli*. There is evidence to suggest that only the small subunit is catalytic; however, this problem has not yet been studied from the perspective of a residue that has been shown to be involved in catalysis.

References

1. Blankenfeldt, W., Asuncion, M., Lam, J. S., and Naismith, J. H. (2000) *EMBO J.* **19,** 6652-6663.

2. Brown, K., Pompeo, F., Dixon, S., Mengin-Lecreulx, D., Cambillau, C., and Bourne, Y. (1999) *EMBO J.* **18,** 4096-4107.

3. Binderup, K., Watanabe, L., Polikarpov, I., Preiss, J., and Arni, R. K. (2000) *Acta Crystallogr. D. Biol. Crystallogr.* **56,** 192-194.